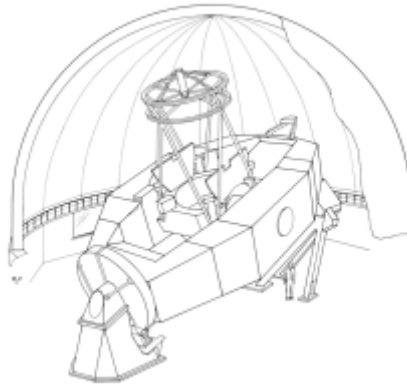




---

## PRELIMINARY DESIGN REVIEW - MECHANISMS -

Original Author: Morgan Bonnet  
Latest Revision: Morgan Bonnet  
Approved by: XX



NASA Infrared Telescope Facility  
Institute for Astronomy  
University of Hawaii

### Revision History

Revision No.	Author & Date	Approval & Date	Description
Revision 1.0	Morgan Bonnet Mar15/13	Morgan Bonnet Mar 15/13	Preliminary Release.



---

## Contents

<b>1 Introduction</b> .....	<b>5</b>
<i>1.1 Project Background</i> .....	<i>5</i>
<i>1.2 Document Purpose</i> .....	<i>5</i>
<i>1.3 Applicable and Reference Documents</i> .....	<i>5</i>
<i>1.4 Abbreviations</i> .....	<i>6</i>
<b>2 Instrument Reference Design</b> .....	<b>7</b>
<i>2.1 Basic Layout</i> .....	<i>7</i>
<i>2.2 Observing Modes and Calibration</i> .....	<i>9</i>
<i>2.3 Acquisition and Guiding</i> .....	<i>9</i>
<b>3 ISHELL Mechanisms Overview</b> .....	<b>10</b>
<b>4 Choice of a Standard Bearings Mount</b> .....	<b>11</b>
<b>5 Discrete Angular Position Mechanisms</b> .....	<b>14</b>
<i>5.1 Choice of a type of wheel mechanism:</i> .....	<i>14</i>
<i>5.1.1 Description of the modified Geneva Wheel:</i> .....	<i>15</i>
<i>5.1.2 Torque Calculations</i> .....	<i>17</i>
<i>5.1.3 Wheel Position Control</i> .....	<i>17</i>
<i>5.2 The Slit Wheel / Order Sorting Wheel Mechanism Combo</i> .....	<i>18</i>
<i>5.2.1 The Slit Wheel Mechanism (SLM)</i> .....	<i>21</i>
<i>5.2.2 The Order Sorting Wheel Mechanism (OSM)</i> .....	<i>23</i>
<i>5.3 The Filter Wheel Mechanism (FWM)</i> .....	<i>25</i>
<i>5.3.1 Optical Elements</i> .....	<i>25</i>
<i>5.3.2 Configuration of the Filter wheel:</i> .....	<i>26</i>
<i>5.3.3 Optical Elements mount:</i> .....	<i>27</i>
<i>5.4 The Cross-Disperser Mechanism (XDM): Grating Selection</i> .....	<i>29</i>
<i>5.4.1 Optical Elements</i> .....	<i>29</i>
<i>5.4.2 Grating Modules</i> .....	<i>32</i>
<b>6 Continuous Angular Position Mechanisms</b> .....	<b>33</b>
<i>6.1 The Image Rotator (IMR)</i> .....	<i>33</i>
<i>6.1.1 Design Description:</i> .....	<i>33</i>
<i>6.1.2 K-Mirror Assembly:</i> .....	<i>34</i>
<i>6.1.3 Drive and Control:</i> .....	<i>35</i>
<i>6.1.4 Anti-Backlash Feature:</i> .....	<i>35</i>
<i>6.2 The Cross-Disperser Mechanism (XDM): Grating Tilt</i> .....	<i>37</i>
<i>6.2.1 Design Description:</i> .....	<i>37</i>
<i>6.2.2 Tilt Drive:</i> .....	<i>37</i>
<i>6.2.3 Tilt Angle Control:</i> .....	<i>38</i>
<b>7 Discrete Linear Position Mechanisms</b> .....	<b>40</b>
<i>7.1 The Dekker Concept:</i> .....	<i>40</i>
<i>7.1.1 Mask Dimensions</i> .....	<i>40</i>
<i>7.1.2 Original Concept: Miniature X-stage</i> .....	<i>40</i>



---

Figure #XXX: MICOS PPS-20 cryogenic piezo X-stage .....	41
7.1.3 <i>Alternative Concept:</i> .....	44
<b>7.2 <i>The Immersion Grating (IG) Mechanism</i></b> .....	<b>45</b>
7.2.1 <i>Immersion Gratings Mounts Concept</i> .....	46
7.2.2 <i>In/Out Fold Mirror Concept</i> .....	47
<b>8 Continuous Linear Position Mechanisms</b> .....	<b>53</b>
<b>8.1 <i>The Spectrograph Detector Focus Stage</i></b> .....	<b>53</b>



## 1 Introduction

### 1.1 Project Background

ISHELL is to be a facility-class infrared cross-dispersed spectrograph developed for the IRTF using silicon immersion grating technology. As a goal, this instrument will provide a resolving power of up to 80,000 at 1.2–2.5  $\mu\text{m}$  and 70,000 at 3–5  $\mu\text{m}$ . No other spectrograph in the Northern Hemisphere presently provides such a high resolving power at near infrared wavelengths.

Silicon immersion gratings are to be incorporated into the design to keep ISHELL manageably small (about the same size as the IRTF facility instrument, SPEX). The immersion grating design will have the advantage of allowing high spectral resolving power without requiring an extremely narrow slit or large collimated beam diameters. This will be the first facility instrument at 1–5  $\mu\text{m}$  to employ an immersion grating, and therefore it will be an important demonstration of this new technology for future instrumentation.

The total instrument budget for ISHELL has been secured from several different sources – NSF, NASA, UH, and through the IRTF operations budget itself. The total budget of the instrument is approximately \$4M and it has been estimated to require about 14 man years of effort (distributed over 4 years) to reach completion.

### 1.2 Document Purpose

XXXXXXXXXXXXXXXXXXXXXXXXXXXXXXXXXXXX

### 1.3 Applicable and Reference Documents

Document Title	Document Number
Operational Concepts Definition Document (OCDD)	
Functional & Performance Requirements Document (FPRD)	
Subsystems Definition Document	
Requirements Document	



---

*1.4 Abbreviations*


---

## 2 Instrument Reference Design

A general description of the instrument is given here as a basis for discussion. This description can be considered as a pre-conceived instrument concept or “strawman design” from which further refinements and/or developments shall occur. It is presented only to give the reader a general flavor of the instrument, and the description given in this reference design should not be interpreted as any kind of established development or requirement of the instrument.

### 2.1 Basic Layout

The ISHELL cryostat is mounted on the telescope at the cassegrain focus. At this focus location the beam speed is approximately  $f/38$ . Inside the cryostat are three major optical sub-assemblies: the fore-optics, the slit viewer, and the spectrograph. The last major subsystem exists outside the cryostat – the calibration unit.

In the fore-optics the  $f/38$  beam from the telescope enters the cryostat through the entrance window and comes to a focus at the telescope focal plane. A dichroic just inside the entrance window transmits the optical beam out of the cryostat through the exit window and into a wavefront sensor, and the infrared beam is reflected. The telescope focal plane is re-imaged onto the slit wheel by a collimator-camera system. A pupil image is formed following the collimator mirror and the system cold stop is placed here. A k-mirror image rotator is located immediately behind the cold stop.

Reflective slits in the slit wheel send the field surrounding the slit into the slit viewer. Here a refractive collimator-camera re-images the slit field onto a Raytheon 512x512 InSb array. A filter wheel in the slit viewer allows a selection of filters to be used for object acquisition, guiding, and scientific imaging. A lens in the filter wheel is used to image the telescope pupil. This pupil viewer provides a means to align the cryostat on the telescope. The slit viewer will operate independently of the spectrograph.

The  $f/38$  beam enters the spectrograph through the slit and order-sorting filter wheel. It is then folded and collimated at the first off-axis parabola (OAP1). The silicon immersion grating is located at the pupil following OAP1. An in/out mirror close to the pupil is able to select either of two immersion gratings (IG1 covers 1.1-2.5  $\mu\text{m}$  and IG2 covers 2.8-5.3  $\mu\text{m}$ ). The immersion grating is tilted slightly so that the emerging beam is reflected at OAP1 to form a dispersed image of the slit at the spectrum mirror. The beam reflected at the spectrum mirror is re-collimated at OAP2 and forms a second “white” pupil image at the cross-disperser mechanism. Gratings in the cross-disperser wheel send the beam into the spectrograph camera lens, which images the resulting spectrum onto a 2048x2048 H2RG array.

A calibration unit is located on top of the cryostat. It contains illuminating optics, an integrating sphere, arc and flat-field lamps, and a gas cell. An in-out mirror above the entrance window is used to project calibration light into the instrument. A gas cell is mounted on a two-position

stage between the entrance window and in-out mirror so that it can be placed into the beam for radial velocity science observations. An option for precision wavelength calibration required for radial velocity science is to feed the output of a laser frequency comb into the integrating sphere. Due to its size ( $\approx 1\text{m}^3$ ) and stability required, the laser comb is located in the instrument preparation room and its output fed to the integrating sphere via an optical fiber.

The cryostat is of similar size to the existing IRTF instrument SPEX ( $\approx 1\text{m}^3$ ) and will nominally uses the same cooling scheme. It contains an optical bench to which the optical sub-assemblies are mounted. The optics and bench are cooled to  $\approx 75\text{K}$  using a liquid nitrogen can. The radiation load on the cold structure is minimized by surrounding it with a radiation shield, which is cooled using the first stage of a Cryodyne 1050 CP closed-cycle cooler. The spectrograph and slit viewer arrays are cooled to  $38\text{K}$  and  $30\text{K}$  respectively, using the second stage of the cooler.

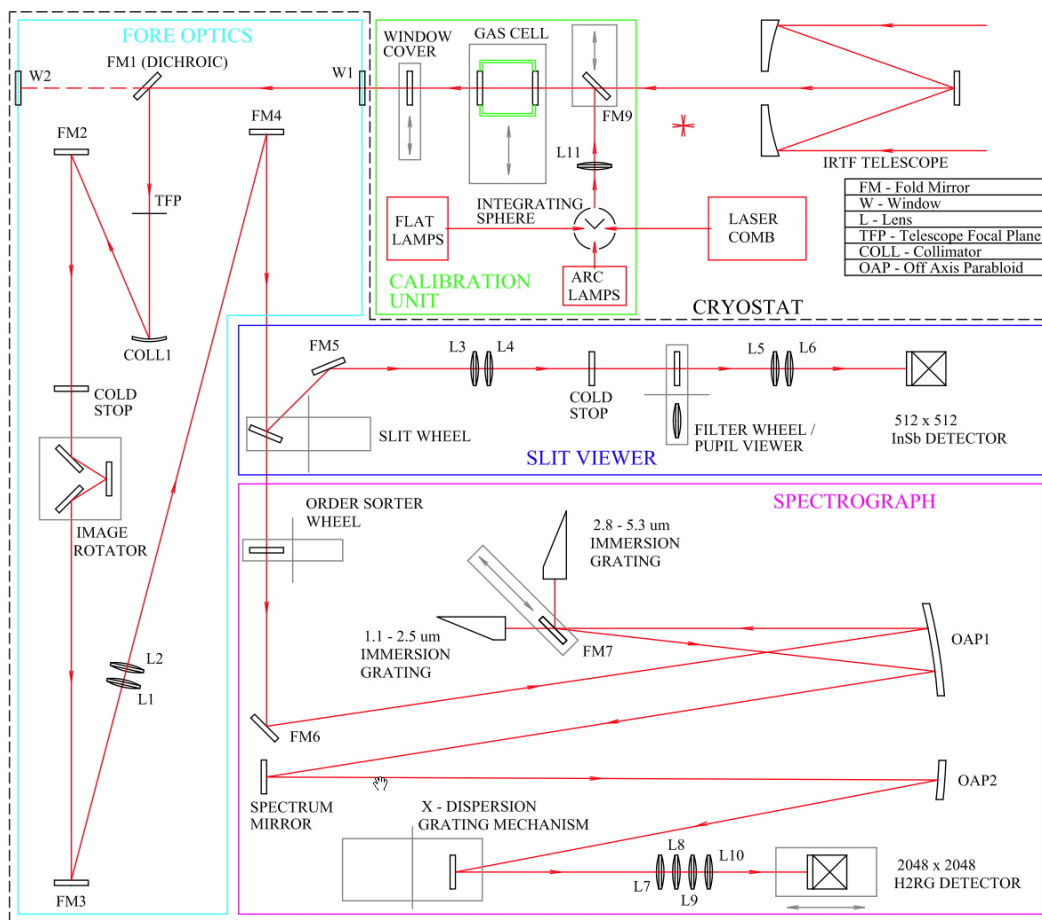


Figure #1: ISHELL schematic layout

---

## ***2.2 Observing Modes and Calibration***

ISHELL has three basic spectroscopy modes. Short cross-dispersed mode covers observations done at  $\sim 1\text{-}2.5\ \mu\text{m}$ . Radial velocity mode is a subset of sort cross-dispersed mode in which observations are made through a gas cell. Long cross-dispersed mode covers observations done at  $\sim 2.8\text{-}5.3\ \mu\text{m}$ . In addition, the infrared slit viewer that is used for acquisition and guiding, can also be used for scientific imaging.

## ***2.3 Acquisition and Guiding***

Target acquisition and guiding is executed with the infrared slit viewer. Due to the high background at wavelengths longer than  $\sim 2.5\ \mu\text{m}$  this is usually done in the *J*, *H*, *K*, or similar wavelength narrow-band filters. Once the target is acquired it is placed in the slit by offsetting the telescope and guiding is started. Since guiding is implemented by offsetting the telescope, guiding is necessarily slow and corrects telescope tracking at rates of  $<0.3\ \text{Hz}$ . In most cases guiding will be done on spill-over from the target star in the slit. Alternatively, a guide star in the field of view of the slit viewer can be used. The centroid of extended objects can be guided on by increasing the size of the guide box.

### 3 ISHELL Mechanisms Overview

The table below lists all of iSHELL's mechanisms:

<i>Layout #</i>	<i>Name</i>	<i>Abbrev.</i>	<i>Type</i>	<i># of Discrete Positions</i>
5	Image Rotator	IMR	Continuous Angular Position	N/A
6	Slit Mechanism	SLM	Discrete Angular Position	5 (10)
	Dekker Mechanism	(DEK)	Discrete Linear Position	4
7	Filter Mechanism	FWM	Discrete Angular Position	15
8	Spectrograph Detector Focus Stage	DET	Continuous Linear Position	N/A
9	Order Sorting Mechanism	OSM	Discrete Angular Position	10
10	Immersion Grating Mechanism	IGM	Discrete Linear Position	2
11	Cross-Disperser Mechanism	XDM	Discrete Angular Position	11
			Continuous Angular Position	N/A

---

#### 4 Choice of a Standard Bearings Mount

Bearings mounts in cryogenic environments are generally challenging due to the simple fact that no traditional type of lubrication can be used and because each part of the assembly will thermally contract as the instrument is cooled down at 77K. Also, each different material has a different contraction rate.

For more details on bearings at cryogenic temperatures, see:

- <http://www.not.iac.es/instruments/notcam/bearings.pdf>
- <http://www.mso.anu.edu.au/gsaoui/documentation/sdns/sdn03.10.htm>
- SPIE paper: “*Cryostat Mechanism Design and Fabrication*” by Tony T. Young; Jeffrey W. Douglass; Klaus-Werner Hodapp; Hubert Yamada; Ev Irvin; Louis Robertson (DOI: 10.1117/12.395459)
- ...

A typical example of technical challenge for a bearing mount in a cryogenic environment would be the use of an aluminum hub with stainless steel bearings. If no clearance is available at warm temperature, the bearings would be crushed down by the aluminum hub and possibly lock once cooled down. Also, having a clearance is often not preferred when the mechanism needs to be semi-aligned at warm temperature. Fortunately, other solutions exist:

- 1) Using of wedges to transform the radial contraction into an axial movement. An axial preload registers the mount against a reference.
- 2) Using the same material for the hub and the shaft of the mount than for the bearing races. Then create an interface with the rest of the mechanism (stainless steel to aluminum for ex.).

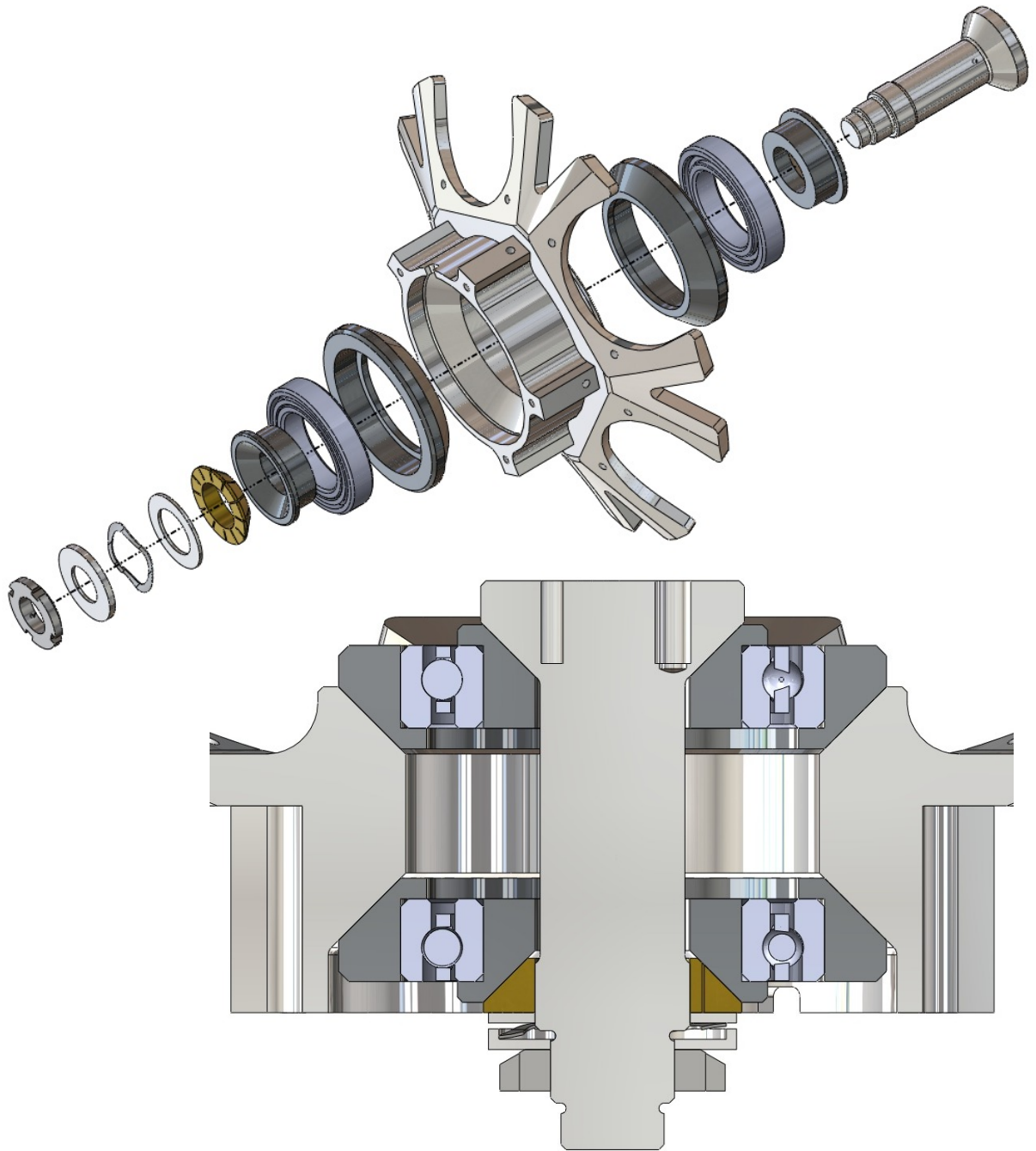


Figure #2: Athermal Bearings Mount – Exploded and Cross-Section Views

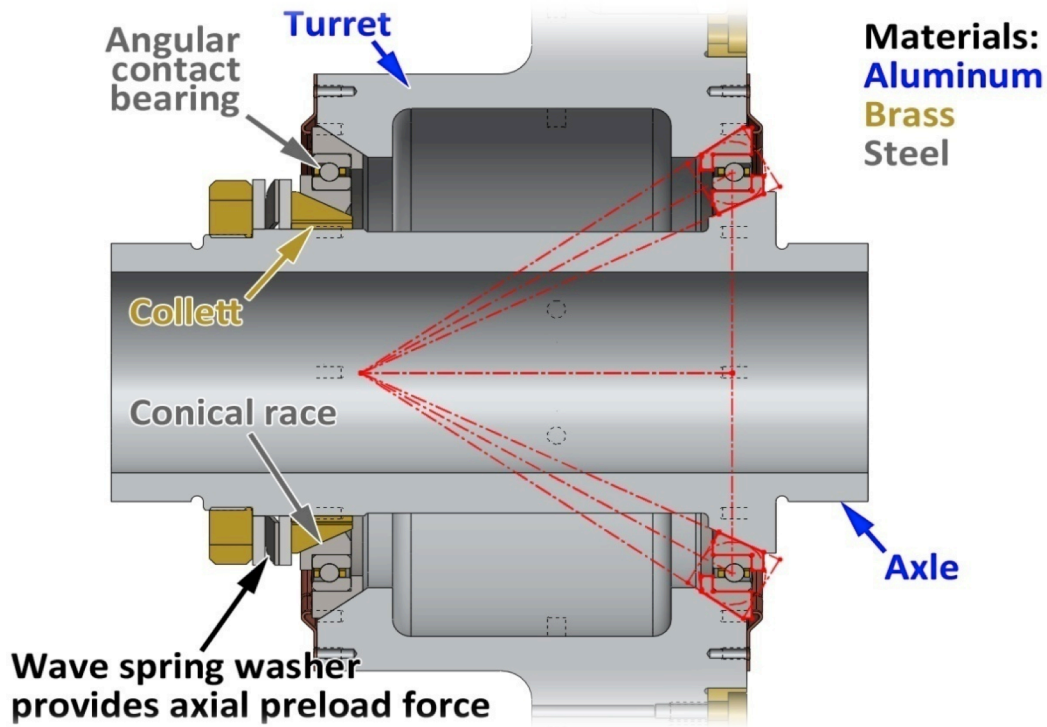


Figure #3: Athermal Bearings Mount – Description

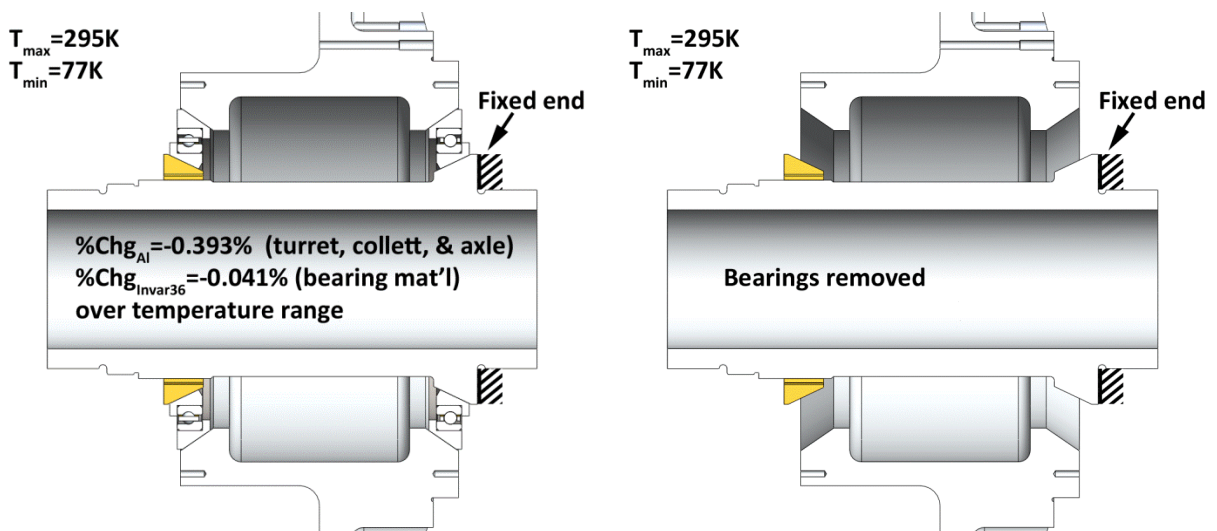


Figure #4: Athermal Bearings Mount – Cool Down Behavior

---

## 5 Discrete Angular Position Mechanisms

### 5.1 Choice of a type of wheel mechanism:

In order to increase the repeatability of Discrete Angular Position mechanisms, it is usually preferable to use a detent to position the wheel in each of its discrete positions, rather than using a low-backlash mechanism with close loop positioning. In addition, for the detent to achieve its purpose properly, the wheel needs to be driven in such a way that it should be compliant, at least close to any of the discrete positions.

To achieve this compliance, there are 2 commonly used drive mechanisms:

- The compliant worm drive
- The Geneva drive

The Compliant worm drive is a worm and wheel type of drive that has its worm compliant to the wheel. The compliance can be achieved through a significant backlash due an important clearance between the worm and the wheel; or it can be achieved by having the worm free to translate (spring loaded) on its rotation axis.

The Geneva drive is designed in such a way that there is a dwell angle around each of the discrete positions (indentations) of the wheel. Once the wheel is within that dwell angle around any discrete position, the detent (released through a cam system) takes over the positioning.

Here is a summary of the pros and cons of a Geneva drive versus a compliant worm drive:

- Pro: Geneva mechanisms locate the wheel close to the required position => less detent force required
- Pro: Geneva mechanisms require less time to index than a worm drive because the reduction ration is usually less
- Con: Geneva mechanisms usually require the use of gear reduction.
- Con: due to the reduction and the use of a cam, Geneva mechanisms have more moving parts than a worm drive
- Pro: Geneva wheels are less expensive to fabricate than worm drives
- Con: Geneva mechanisms are limited in the number of discrete positions.

In order to increase the precision and the repeatability of the Filter Wheel mechanism, a reduced load on the wheel bearings is preferable. The Geneva mechanism has the advantage to support the load of the detent mechanism with its cam when the mechanism is moving from a discrete position to another. In a worm drive, the detent is pushed away by the wheel, which means the load on the wheel is actually even higher outside of the detent positions since the detent spring is compressed further away.

At the light of these considerations but also based on the pros listed above, the Geneva mechanism is the logical choice for the concept of the Filter Wheel.

### 5.1.1 Description of the modified Geneva Wheel:

After working on several concepts, the one presented below corresponds to what we think is the best answer to the challenges of designing a reliable and precise Discrete Angular Position mechanism within the vacuum and cryogenic environment of the instrument. Also, the design has been simplified enough that it should stay relatively easy to implement.

The picture below illustrates the different elements of the Geneva mechanism:

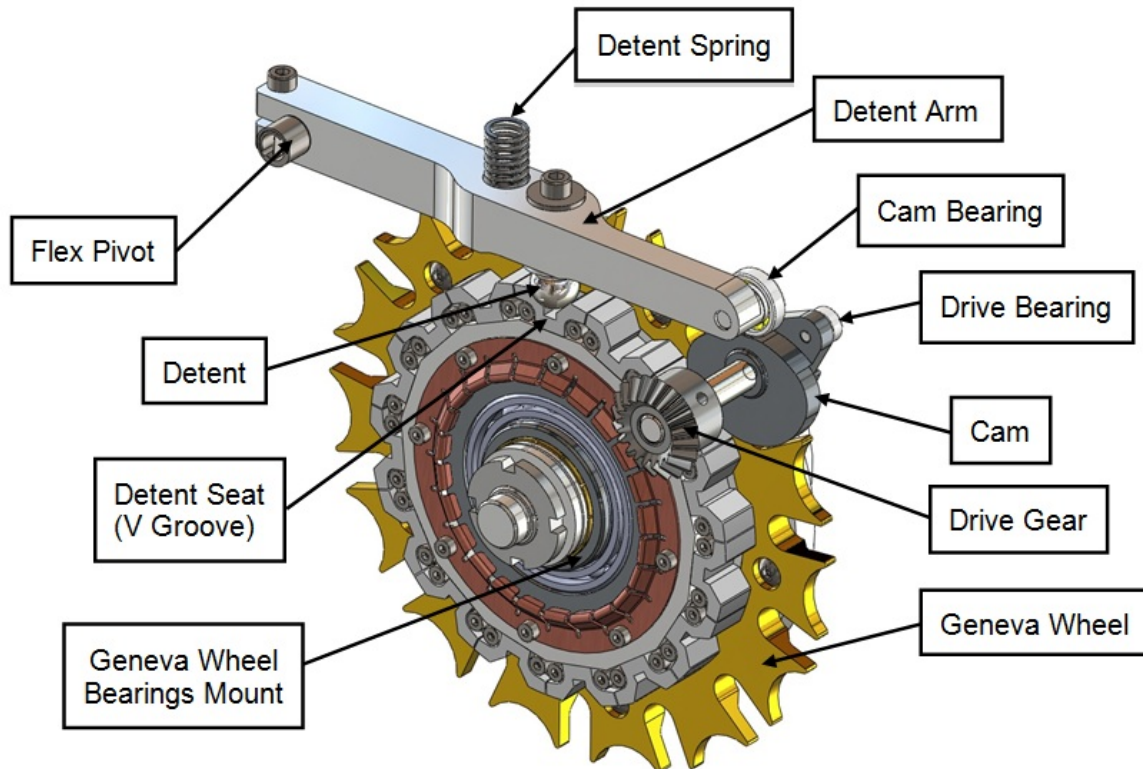


Figure #5: Elements of the modified Geneva mechanism

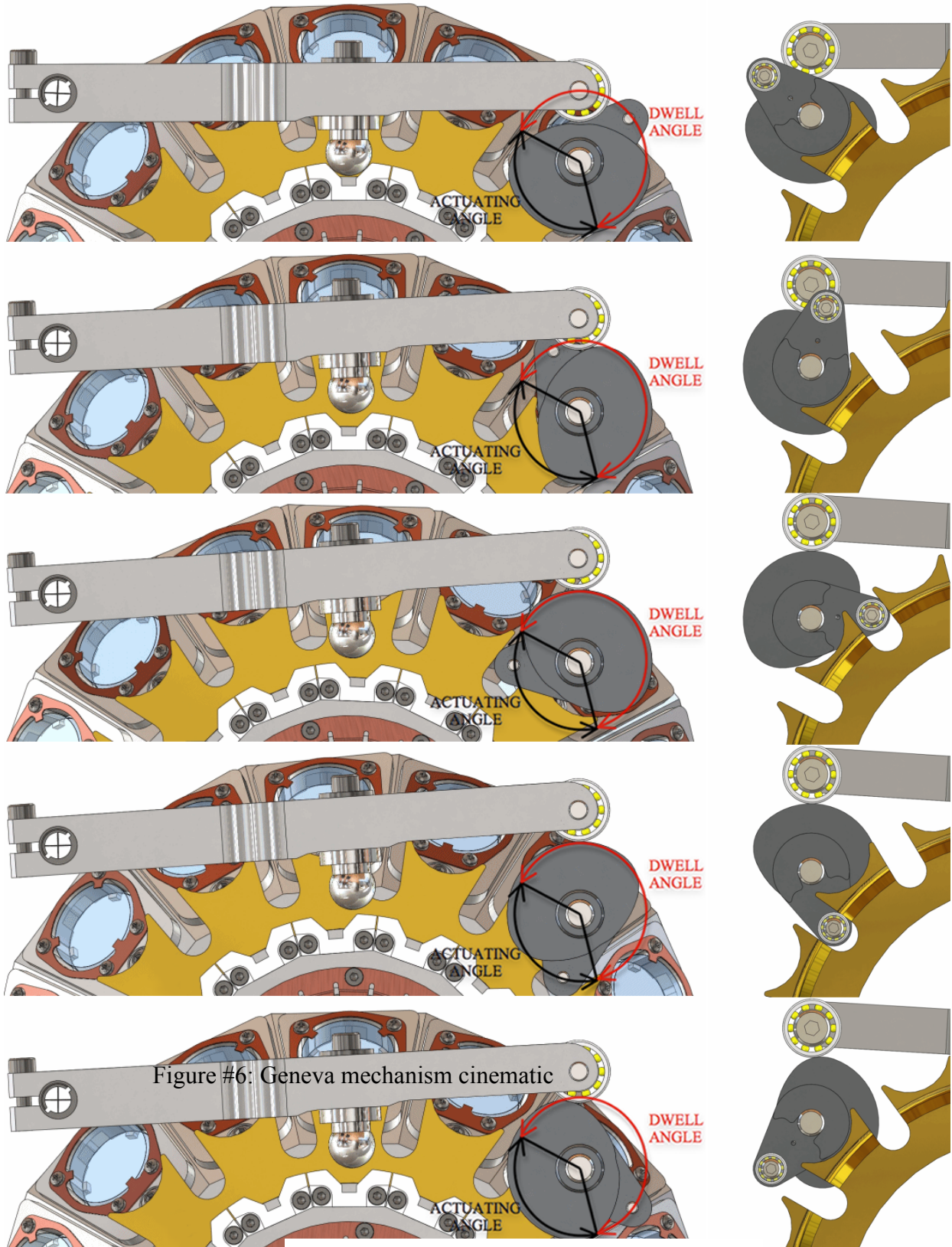
The Geneva mechanism is driven by a cam, which has two functionalities:

- It drives and rotates wheel with the small bearing attached to it,
- It lifts the detent arm from its detent position.

In the detent position, the cam has a deep so that the detent arm is no longer in contact with the cam but only with the detent seat. That way, the force provided by the spring is completely transferred from the cam to the detent seat.

Remark: when the drive bearing disengages from the Geneva wheel, the wheel is still held by the cam even though if the wheel is balanced, it has no reason to move.

For an illustration of the mechanism cinematic, refer to figure #XXX below:



---

### 5.1.2 Torque Calculations

With the modified Geneva wheel design described above, the minimum torque needed at the cam is depending on the force necessary to lift the detent arm (not the force necessary to rotate the wheel) and the “slope” on the cam. This “slope” is directly linked to the required positional time. So the size of the stepper motor and the reduction ratio between the stepper and the cam will be determined by detent force and the required positional time.

#### Notes:

- The choice of a detent force can be tricky to make because on one hand it should be enough to secure the wheel in position but on the other hand it shouldn't be so that it deforms the wheel by an amount that would affect the optical alignment. Also, choosing a force too important might lead to unnecessarily over-sizing the drive.
- The force applied to the detent arm by the spring is at its highest when the arm is in its fully disengaged position, on the greatest diameter of the cam. So the torque necessary to rotate the cam will vary with the position of the cam, and its value will be calculated depending on the spring force and the “slope” of the cam.
- Frictions and efficiency ratios need to be considered in the calculation.

(For more details on the torque calculation, see design note XXX)

### 5.1.3 Wheel Position Control

In addition, to the different elements listed in figure #XXX, a Hall Effect Sensor is needed to sense each of the detent positions. A magnet will be placed at each discrete position and the closest possible of the outside diameter of the wheel.

## 5.2 The Slit Wheel / Order Sorting Wheel Mechanism Combo

The optical layout only provides a limited space for the Slit and the Order Sorting mechanisms. Therefore the configuration of the Order Sorting wheel is strongly dependant on the one of the Slit mechanism (Slit wheel + Dekker combo) and vice-versa. See figure below:

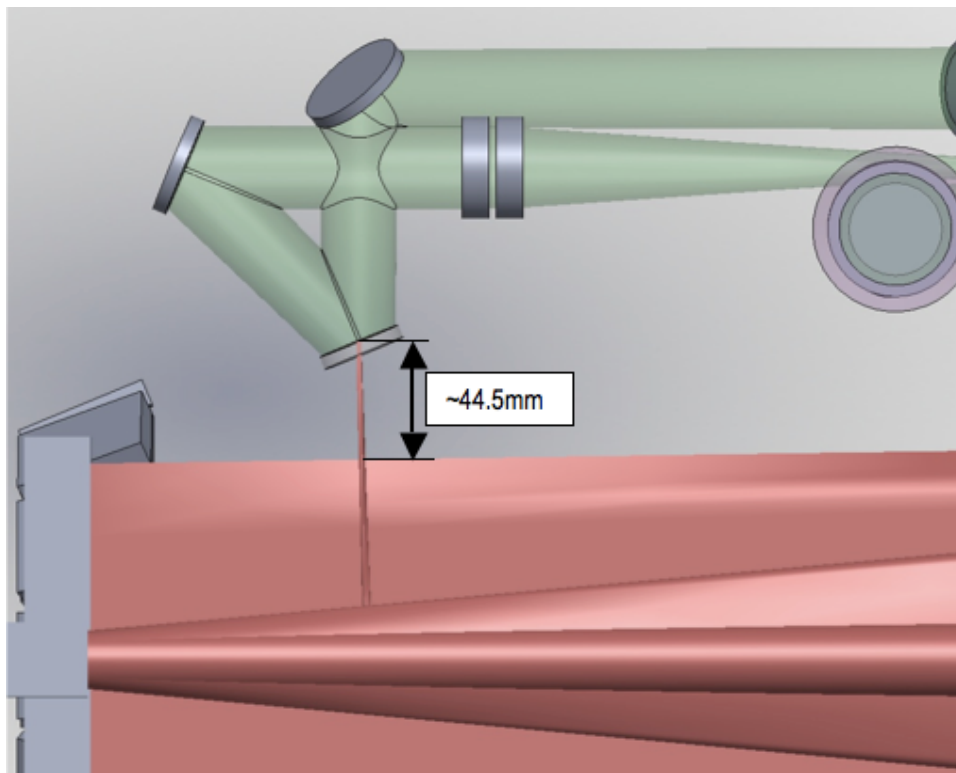


Figure #7: Optical Layout – Space Available

Within the available space, several configurations are possible for the two wheels and the Dekker mechanism. However, the relative position of the mechanisms shall be fixed: the beam will first be split by the Slit Mirror; the part of the beam going through the slit will then be trimmed in length with the Dekker. Next, the beam will continue its way in the spectrograph through the Order Sorter filter. Therefore, to respect that order, the Dekker mechanism should be placed between the 2 wheels.

Also, in order to comply with the optical requirements, the Dekker should be no further than 10mm from the Slit. But since the Slit mirror element will effectively be a 5mm thick substrate, the front face of the Dekker mask should be no further than 5mm away from the Slit Mirror substrate, and ideally the closest possible.

Additionally, on top of the space limitation due to the optical layout, it was necessary to leave a significant amount of space for the Cross-Disperser mechanism, which is the biggest mechanism of the instrument. (See 5.4 and 6.2)

In an earlier concept the 2 wheels were angled at 22.5 degrees from each other with the Dekker mechanism located in the middle. (See Figure #XXX)

With that configuration, for space saving reasons, the two wheels had to be mounted on a common stainless steel bearings hub. The Dekker stage was mounted on that hub as well. Also, in order to have the 2 bearing hubs clear each other, the Order Sorting wheel diameter had to be bigger.

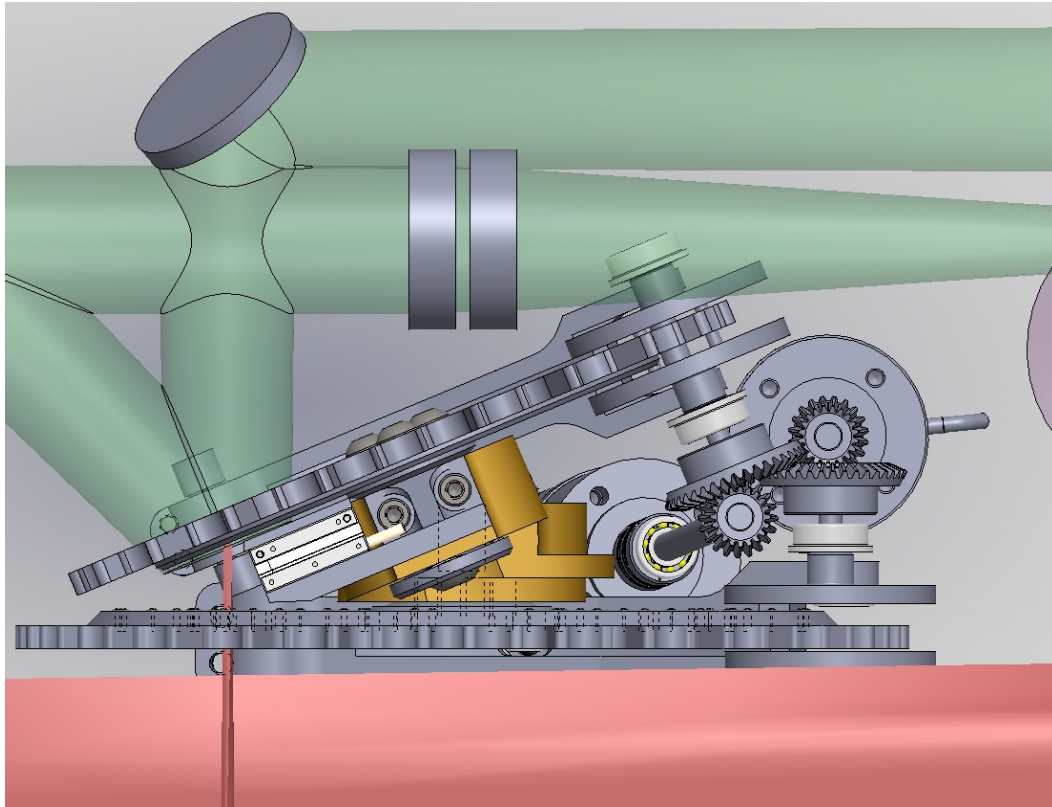


Figure #8: Slit and Order Sorter Mechanisms Combo – Earlier Concept

At the end, we decided not to pursue this concept further because it required having the 2 mechanisms (3 with the Dekker) mounted on a common hub, which would probably have been an issue when aligning the instrument with that configuration.

A better concept then, was to have the 2 wheels parallel to each other, mounted on each side of the bench and separated with a thin plate to avoid light leaks from the fore-optics to the spectrograph side of the instrument. In that configuration, the Slit Wheel has to have a conical shape with a 22.5deg angle in order to position the Slit Element properly.

But because of the extreme limited amount of space allocated for the Slit and Order Sorting mechanisms, it turned out to be necessary to have them intricate into each other. See Figure below:

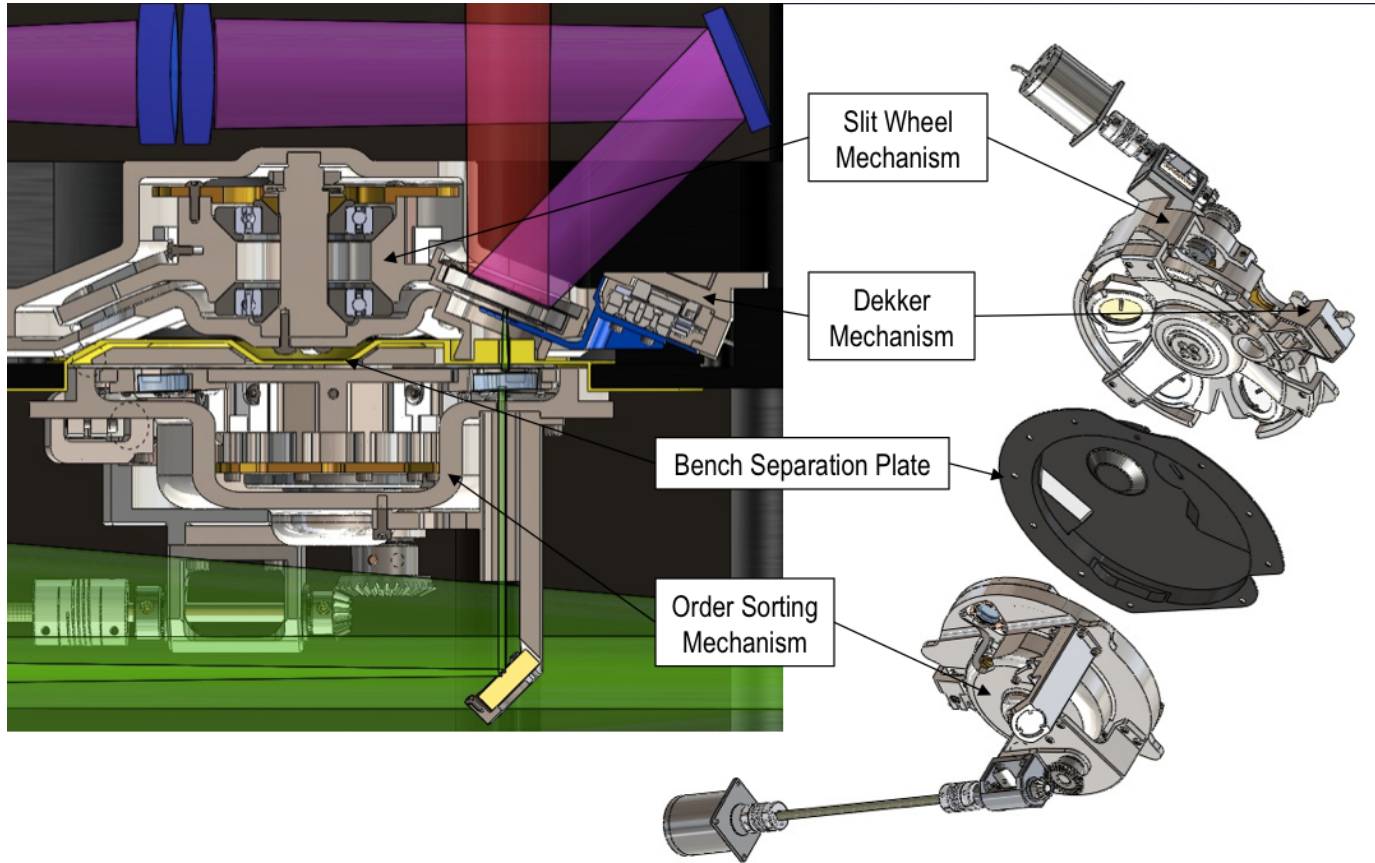


Figure #9: Slit and Order Sorter Mechanisms Combo

5.2.1 The Slit Wheel Mechanism (SLM)

5.2.1.1 Number of Discrete Positions:

A minimum compliment of slits required has been identified below:

<b>Position #</b>	<b>Slit width</b>	<b>Slit length</b>	<b>R</b>
1	0.375"	5.0"	72,000
2	0.375"	10.0"	72,000
3	0.375"	15.0"	72,000
4	0.375"	25.0"	72,000
5	0.75"	5.0"	39,000
6	0.75"	10.0"	39,000
7	0.75"	15.0"	39,000
8	0.75"	25.0"	39,000
9	1.50"	5.0"	20,000
10	1.50"	10.0"	20,000
11	1.50"	15.0"	20,000
12	1.50"	25.0"	20,000
13	3.00"	5.0"	10,000
14	3.00"	10.0"	10,000
15	3.00"	15.0"	10,000
16	3.00"	25.0"	10,000
17	Blank-off/mirror (darks/slit-less imaging)		

The total number of discrete positions required in the slit mechanism is 17.

With the use of a Dekker mechanism, the Slit mechanism is split in 2 parts: a slit wheel and a Dekker stage.

The slit wheel is defining the slit widths whereas the Dekker stage is defining the slit lengths. In addition the slit wheel contains a blank-off/mirror position. When the slit mechanism is used in that position, the Dekker stage has no functionality and therefore its position has no influence.

The 17 positions are realized as follow:

$$[\text{Dekker Stage (4 width)}] \times [\text{Slit Wheel (4 length)}] + [\text{Slit Wheel (mirror)}] = 17 \text{ positions}$$

<b>Slit Wheel</b>		
<b>Position #</b>	<b>Slit width (Arcsec)</b>	<b>Slit width (mm)</b>
1	0.375	0.207
2	0.75	0.415
3	1.50	0.829
4	3.00	1.658
5	Blank-off/mirror	Blank-off/mirror

<i>Dekker Stage</i>		
<i>Position #</i>	<i>Slit length (Arcsec)</i>	<i>Slit length (mm)</i>
1	5	2.763
2	10	5.527
3	15	8.29
4	25	13.817

(Note: the conversion from arcsec to mm is using the following conversion rate: 1.8093'/mm.)

Remark: This part of the document will only describe the Slit wheel part. For the Dekker, refer to (7.1).

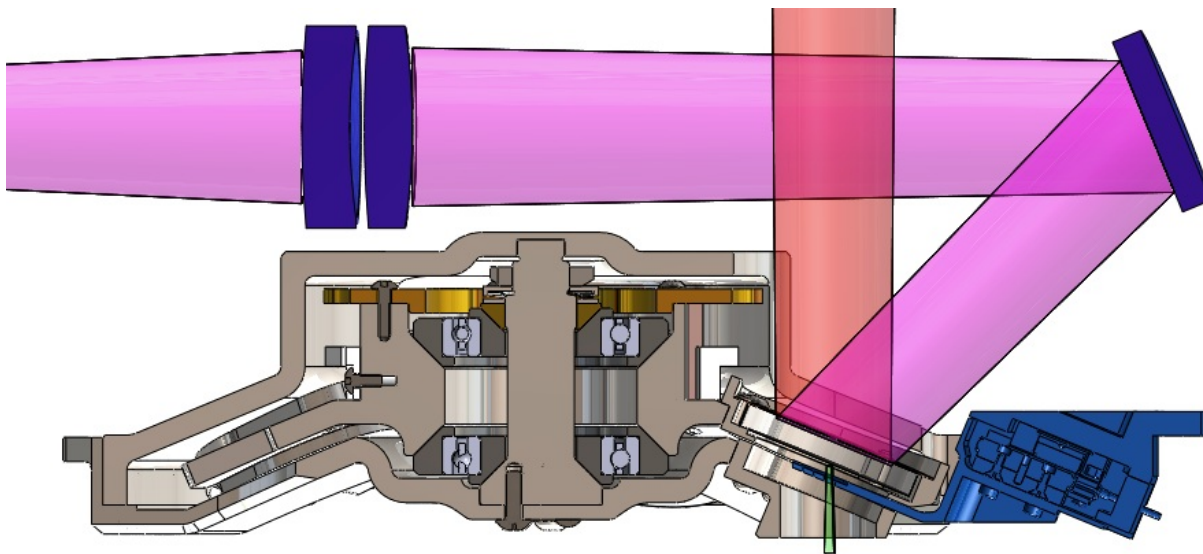


Figure #10: Slit Wheel – Cross-Section

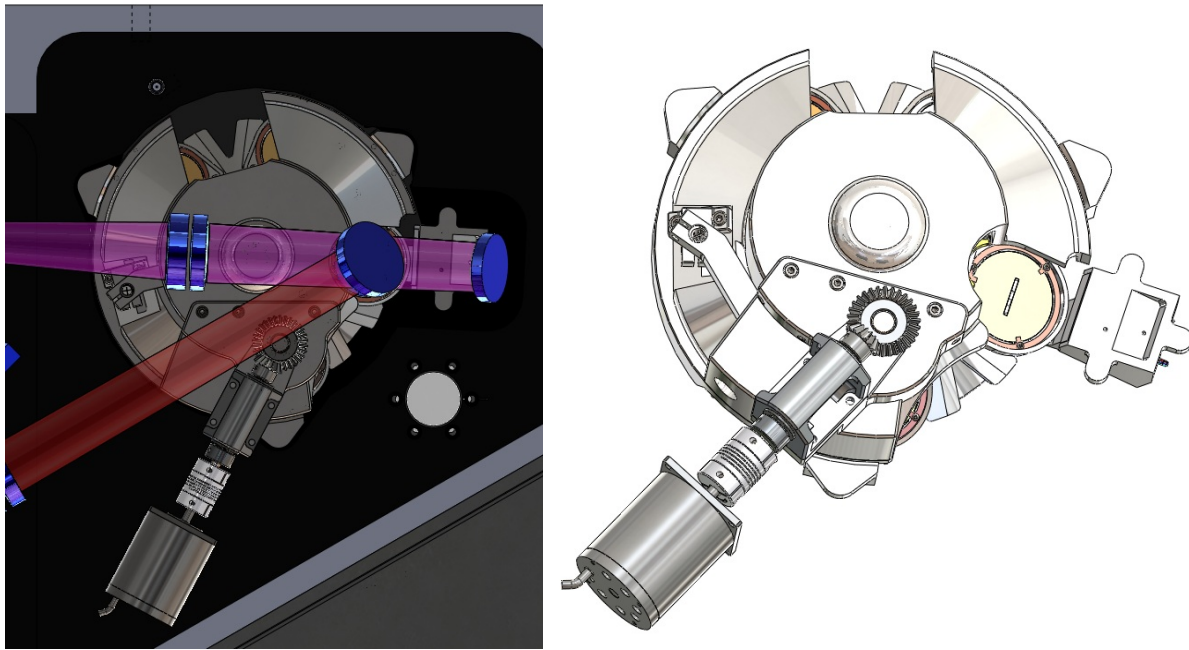


Figure #11: Slit Wheel Description

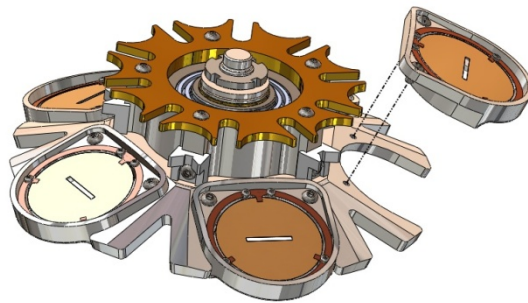


Figure #12: Slit Wheel Turret and Optical Element Mount

### 5.2.2 *The Order Sorting Wheel Mechanism (OSM)*

The optical design calls for a filter element in the spectrograph, right after the Slit (see figure #1). In reality, this element will need to be interchanged from a selection of elements for different observing scenario. The concept being that any of the filter selection (or possibly, no filter at all) may be chosen for an observation.

#### 5.2.2.1 Number of Discrete Positions:

A minimum compliment of filters required has been identified below:

<i>Filter</i>	<i>Notes</i>
<i>Blank-off</i>	
<i>J-band XD</i>	1.05-1.45 $\mu$ m
<i>H-band XD</i>	1.40-1.90 $\mu$ m
<i>K-band XD</i>	1.80-2.60 $\mu$ m
<i>L/L'-band XD</i>	2.70-4.20 $\mu$ m

<i>Filter</i>	<i>Notes</i>
<i>M-band XD</i>	4.50-5.50 $\mu$ m
<i>Single Order</i>	TBD
<i>Single Order</i>	TBD
<i>Single Order</i>	TBD
<i>Open</i>	

The total number of discrete positions required in the filter mechanism is 10.

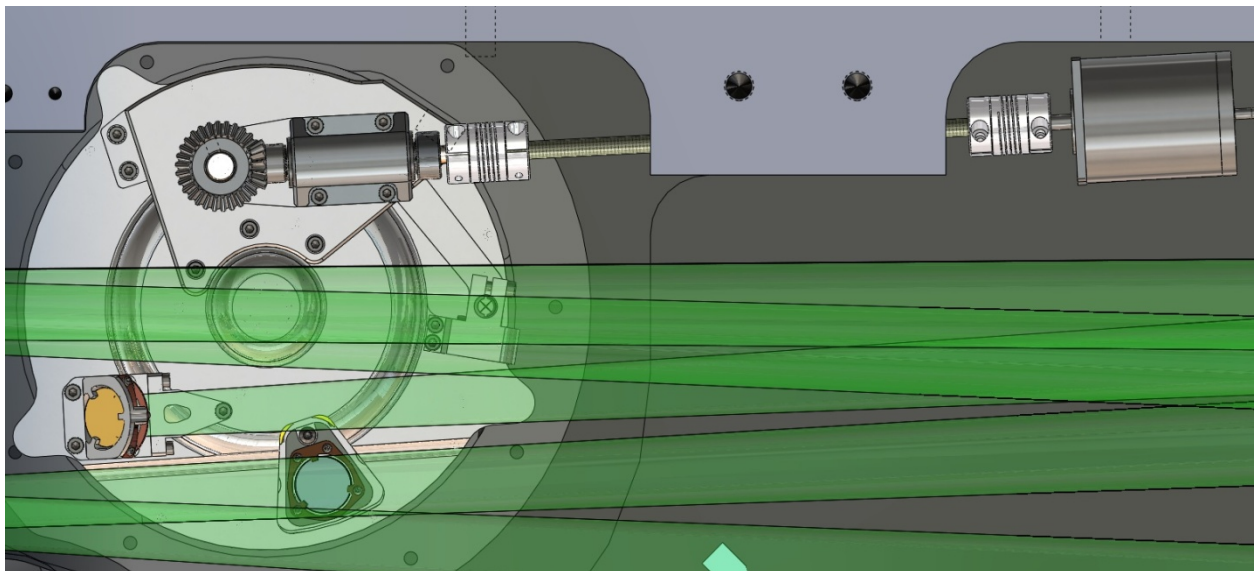


Figure #13: Order Sorting Wheel on the Bench

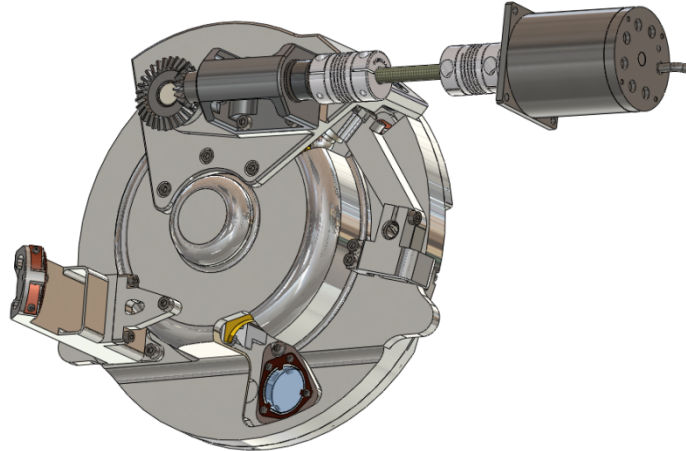


Figure #14: Order Sorting Wheel - Isometric View

### ***5.3 The Filter Wheel Mechanism (FWM)***

The optical design calls for a filter element, prior to the last set of camera optics in the slit viewer (see figure #1). In reality, this element will need to be interchanged from a selection of elements for different observing scenario. Also included in this position is a specialized element to be used for pupil viewing. The concept being that any of the filter selection (or possibly, no filter at all) may be chosen for an observation, or the pupil viewing element may be moved into position for image quality / engineering purposes.

#### ***5.3.1 Optical Elements***

Number of Elements:

- 14 Filters
- 1 Pupil Viewer

Dimensions of the Elements:

- Filters:  $19.05 \pm 0.05$  mm in diameter and  $5.00 \pm 0.05$  mm in thickness
- Pupil Viewer:  $19.05 \pm 0.05$  mm in diameter and  $5.00 \pm 0.05$  mm in thickness

### 5.3.2 Configuration of the Filter wheel:

With the filter wheel having a rather high number of discrete positions, and since iSHELL's optical layout is driving a compact instrument, the use of an usual "flat" wheel would have been taking too much space, especially when also considering the assumed volume occupied by the other mechanisms in the instrument.

For that reason, we investigated different configurations possible for the filter wheel. It appeared that a "conical" 45 degrees type of wheel was the more appropriate, since it drastically reduces the overall diameter of the wheel.

Also, instead of having the Geneva wheel on the outside diameter of the Filter Wheel, another space saving feature of the Filter mechanism was to attach the Geneva wheel on the back of the filter wheel (See Figure #XXX).

The diameter of the Geneva wheel was chosen so that it is as big as possible in order to increase the precision of the detent, but small enough so that it would clear the light beam (See Figure #XXX).

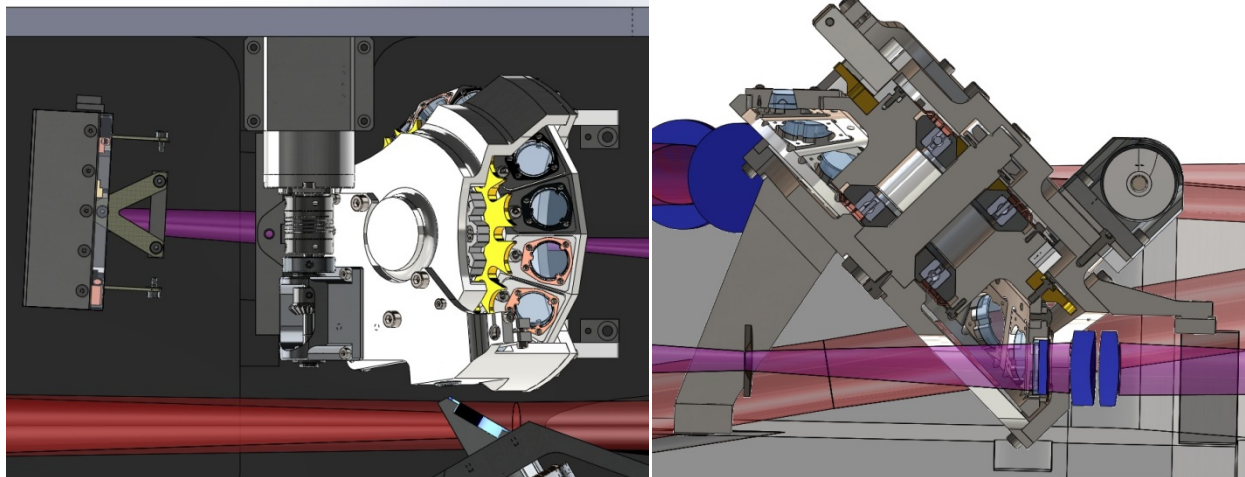


Figure #15: Filter Wheel on the Bench – Side and Section Views

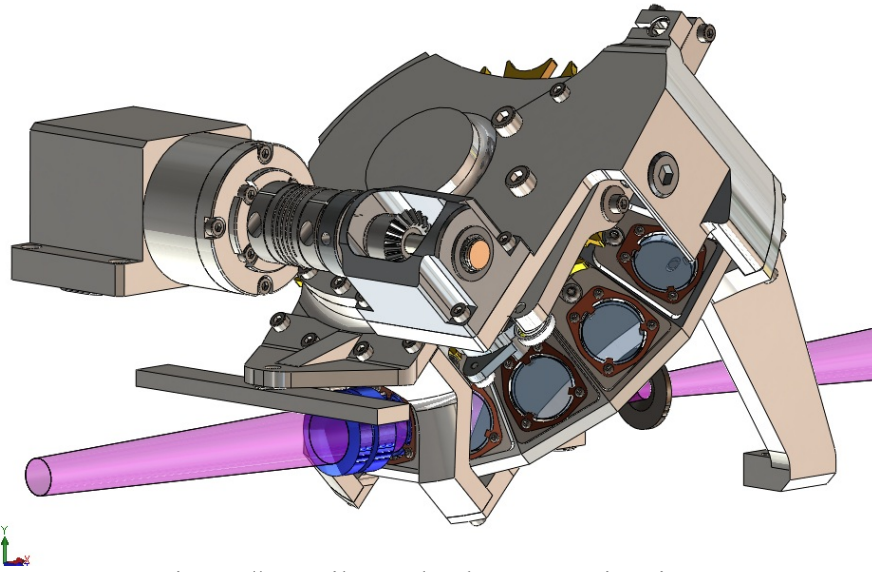


Figure #16: Filter Wheel – Isometric View

5.3.3 *Optical Elements mount:*

Filter Cell:

In order to facilitate changing filters, it is usually a good solution to use a filter cell. The cell in the picture below is reusing the same concept as the one use for the filter wheel of SpeX:

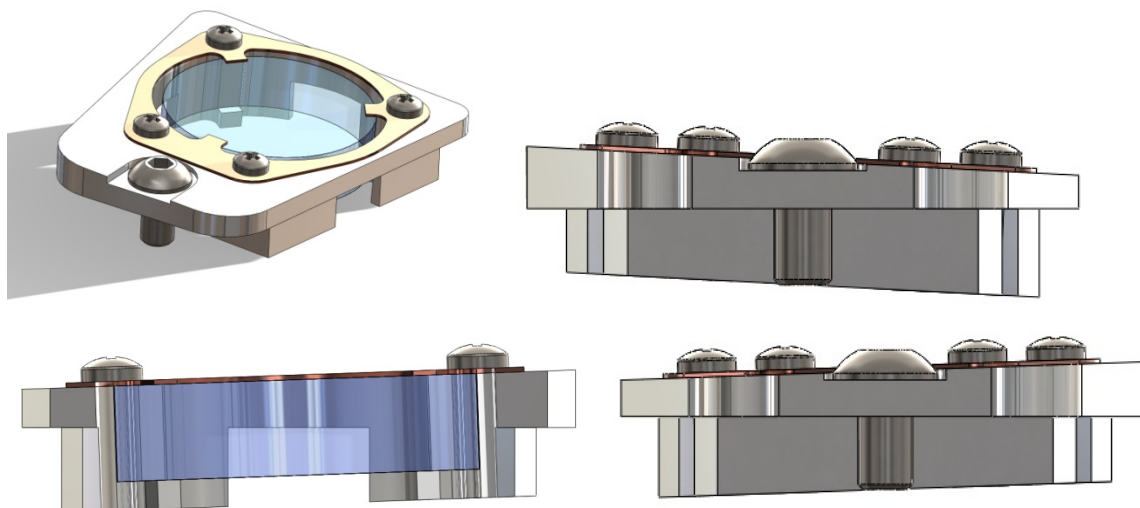


Figure #17: Filter Wheel – Optical Element Mounts



Note: one difference with SpeX's filter cell is that in order to improve the positioning of the filter in the cell, the filter is now being registered using 3 "feet" at 120 degrees instead of a ring. This allows the filter to be statically determinate.

Filter Orientation:

Another advantage of having the Filter Wheel with a 45 degrees "conical" shape is the access to the filter, for filter changes during the life of the instrument. Instead of having to access along the light path, this orientation allows to access the filters from the side of the instrument. This will facilitate the design of an access cover.

### 5.4 The Cross-Disperser Mechanism (XDM): Grating Selection

The optical design calls for a cross-dispersion grating element in the spectrograph, right after the Off-Axis Parabola #2 (see figure #1). In reality, this element will need to be interchanged from a selection of elements for different observing scenarios. The concept being that any of the XD grating selections may be chosen for an observation.

Note: this section of the document will not treat the mechanism tilt. For the description of the tilt concept, see (6.2)

#### 5.4.1 Optical Elements

The table below describes the grating parameters for each grating module including the exposure names, nominal XD tilt, the deviation from the nominal XD tilt, and the grating dimensions. Note that there are multiple exposure names for some of the modules and in general, each module has a unique average XD tilt and deviation.

Exposure Name	Module	Nominal XD Tilt Angle (Degrees)	Deviation from Nominal XD Tilt (Degrees)	Grating Length (all widths = 40mm)	Custom Grating?
J	1	39.40	+/- 0.00	40	yes
H	2	35.20			yes
K	3	28.00			yes
J1	4	58.75	+/- 2.75	55	no
J2					
H1	5	54.35	+/- 2.75	50	yes
H2					
H3					
K1	6	56.10	+/- 2.40	50	no
K2					
K3	7	54.00	+/- 2.40	50	no
K4					
L1	8	54.30	+/- 3.00	50	yes
L2					
L3					
L4	9	52.35	+/- 3.85	50	no
L5					
L6					
M1*	10	40.40	+/- 0.00	40	no
M2**	11				

Notes:

1. This table was generated by data taken from document "XDs\_28jan11" by John Rayner.
  2. Nominal Tilt Angle is the angle between the incident ray and the grating normal at the XD tilt axis mid travel position.
  3. Each module holds a unique grating except modules 10 & 11, which hold identical gratings.
- \*M1 to be tilted +0.2 deg in the dispersion direction.  
\*\*M2 to be tilted -0.2 deg in the dispersion direction.

### 5.4.2 Configuration of the Cross-Disperser Mechanism

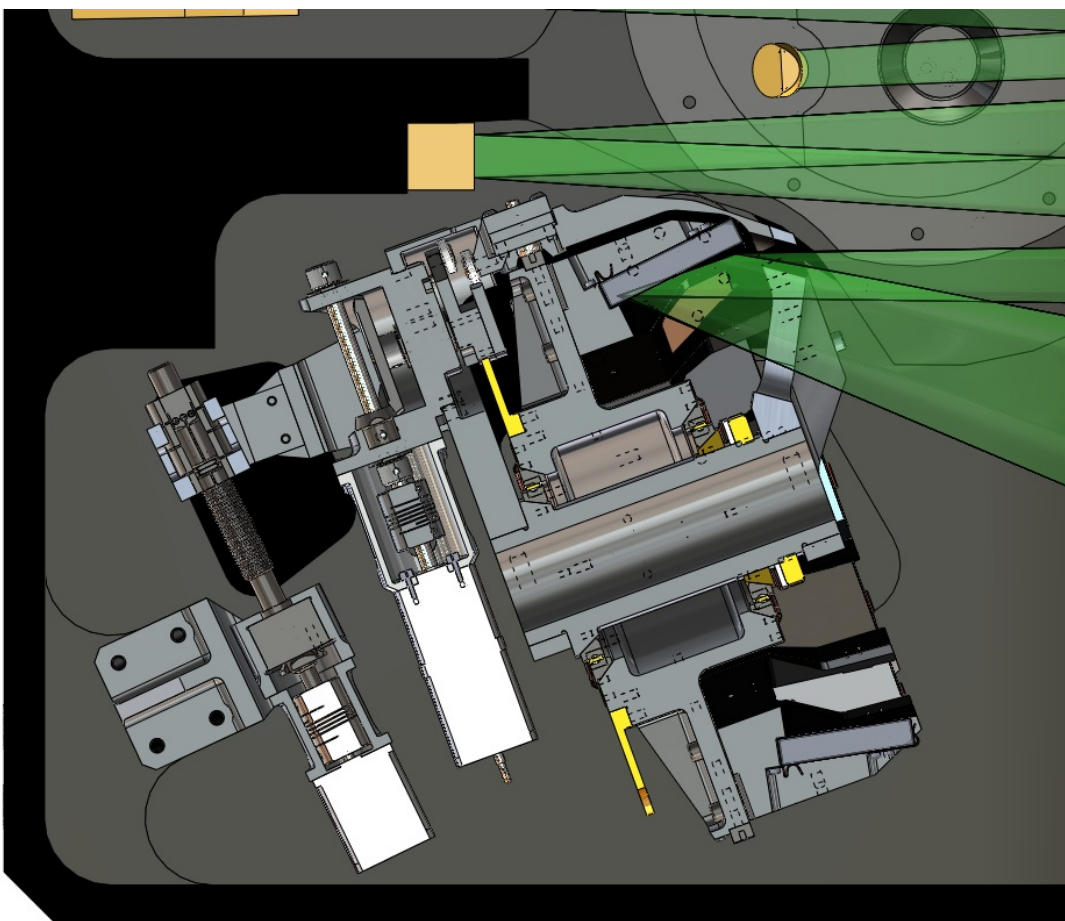


Figure #18 Cross-Disperser Mechanism on the Bench – Side Section View

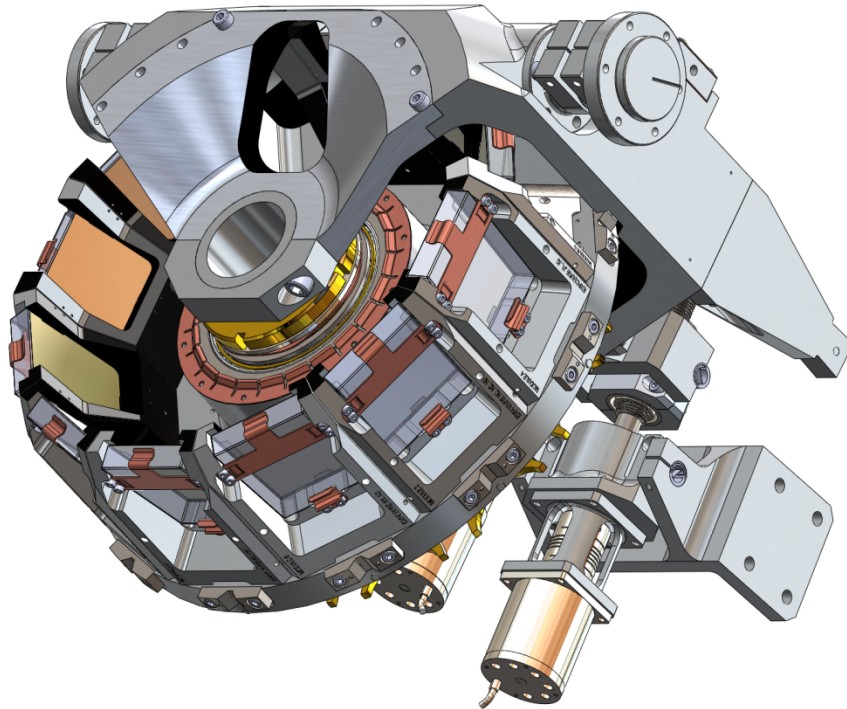


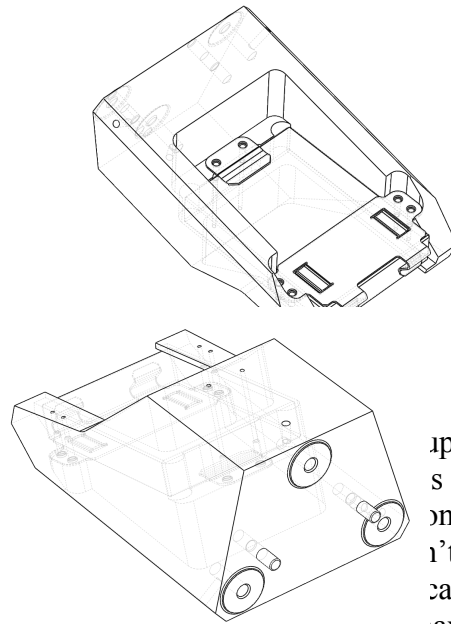
Figure #19: Cross-Disperser Mechanism – Isometric View

---

### 5.4.3 Grating Modules

The cross disperser turret design incorporates the grating. The basic shape of each module is different to accommodate the geometry of the grating.

Each grating is mounted in a module without over constraining it. It should be fully constrained where the sixth unconstrained direction is parallel to the ruling direction of the grating to prevent bending moments or excessive force into the grating. (All contact surfaces between the grating and the module are covered with Teflon) tape interface so that no metal-to-glass contacts exist.)



---

ion grating in  
atures in each  
gles) of each

upport the grating  
s of freedom are  
on in the direction  
it impart bending  
cal performance of  
ave a Kapton (or

Each grating module implements kinematic mounting features to fully constrain all six degrees of freedom and ensure repeatable replacement of the modules onto the turret. Fasteners used to mount the modules to the turret are captive to prevent them from falling into the instrument when removing/installing the modules.

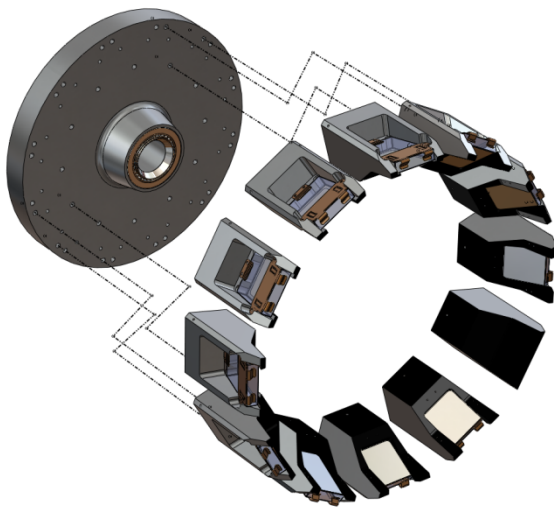


Figure #20: Cross-Disperser Grating Modules

## 6 Continuous Angular Position Mechanisms

### 6.1 The Image Rotator (IMR)

The Image Rotating Mechanism, also commonly called Image Rotator, which allows to continuously rotating the image on the Slit Viewer. The optical design calls for an Image Rotator in the Fore-Optics, right after the Fold Mirror #2 (see figure #1).

#### 6.1.1 Design Description:

The original design was integrating the 2 mirror folds (FM2 and FM3) and the cold stop. However, in order to facilitate the overall Instrument Alignment, it is preferable to align these elements separately from the K-Mirror.

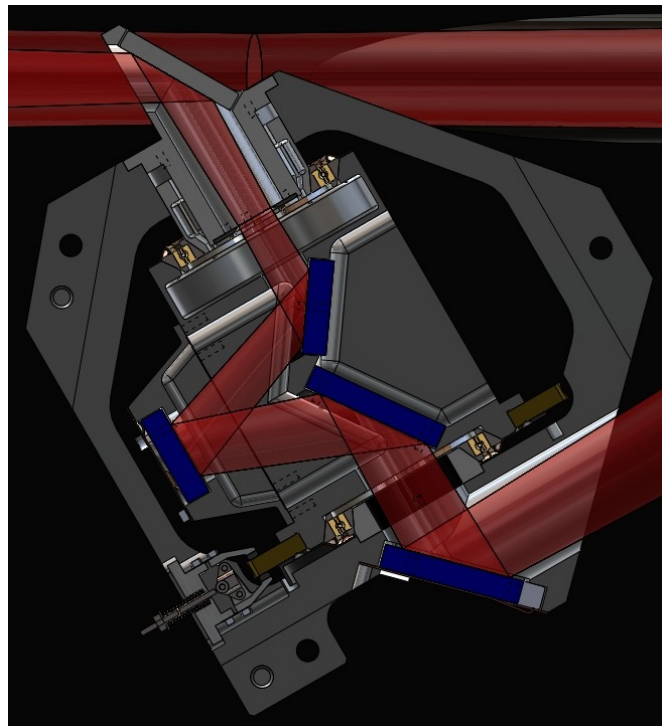


Figure #21: Image Rotator – First Concept

Therefore, a more compact mechanism was designed to separate the Folds and the Cold Stop and leaving enough room for separate mounts at the same time.



d Stop

K-Mirror

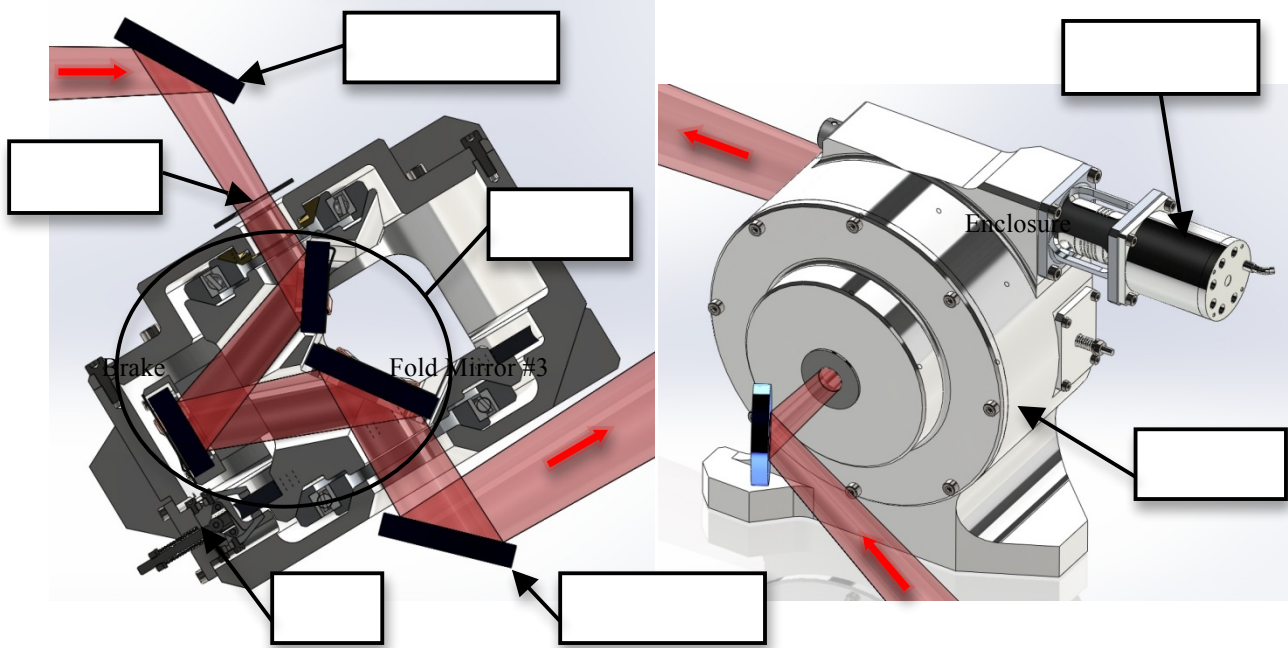


Figure #22: Image Rotator – Cross-Section and Isometric views

6.1.2 K-Mirror Assembly:

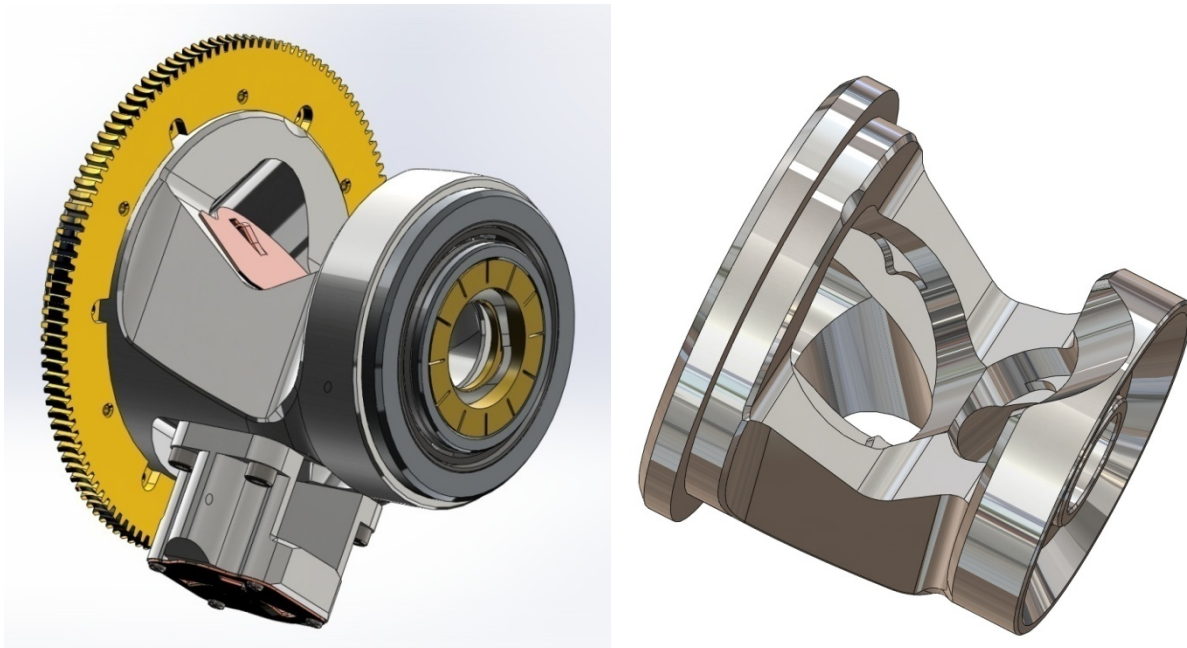
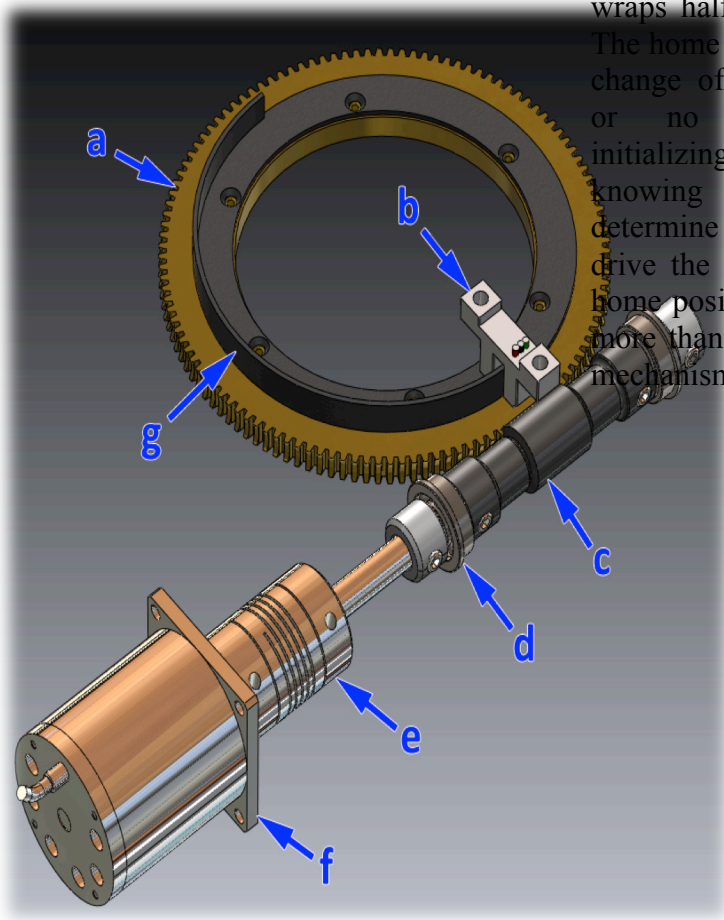


Figure #23: K-Mirror Assembly and Hub

- ISHELL\_PDR\_Mechanisms\_032213.docx  
Created by Morgan Bonnet
- a) 120 tooth brass worm gear
  - b) Hall effect sensor
  - c) Vespel worm
  - d) Drive shaft bearing
  - e) Flex coupling
  - f) Stepper motor

The middle mirror of the K-mirror assembly is separated from the main hub because it would be highly difficult to fabricate as one part.

### 6.1.3 Drive and Control:



The home position sensor is a hall-effect sensor that senses the proximity of a blade. The blade is mounted to the worm gear and wraps half way around the gear. The home position is defined by a change of state: sense/no sense, or no sense/sense. When initializing the mechanism, knowing the initial state will determine which direction to drive the mechanism to find the home position, which requires no more than a half of a turn of the mechanism to find the home.

Figure #24: Image Rotator Drive

### 6.1.4 Anti-Backlash Feature:

The brake straddles the worm gear similar to a bicycle brake and provides a clamping force via a compression spring. The braking force is adjustable by adjusting the compression spring preload. See Figure below:

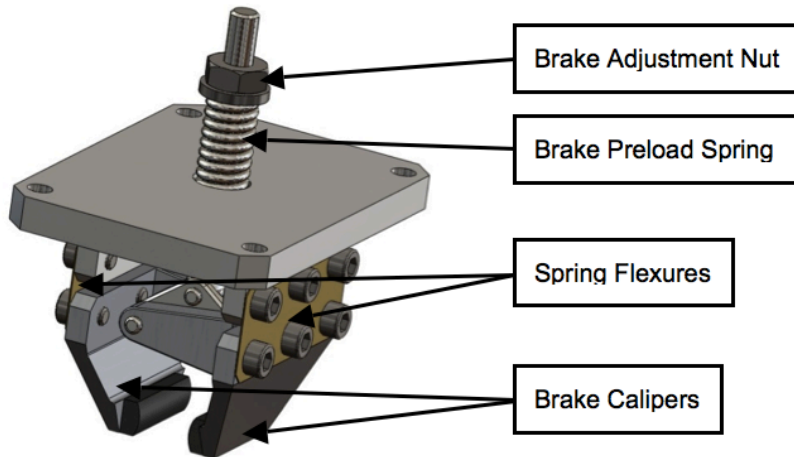


Figure #25: Image Rotator – Anti-Backlash Brake System

Note: another option that could still be implemented would be to use a preloaded worm onto the worm gear like in SpeX's image rotator.

## 6.2 The Cross-Disperser Mechanism (XDM): Grating Tilt

### 6.2.1 Design Description:

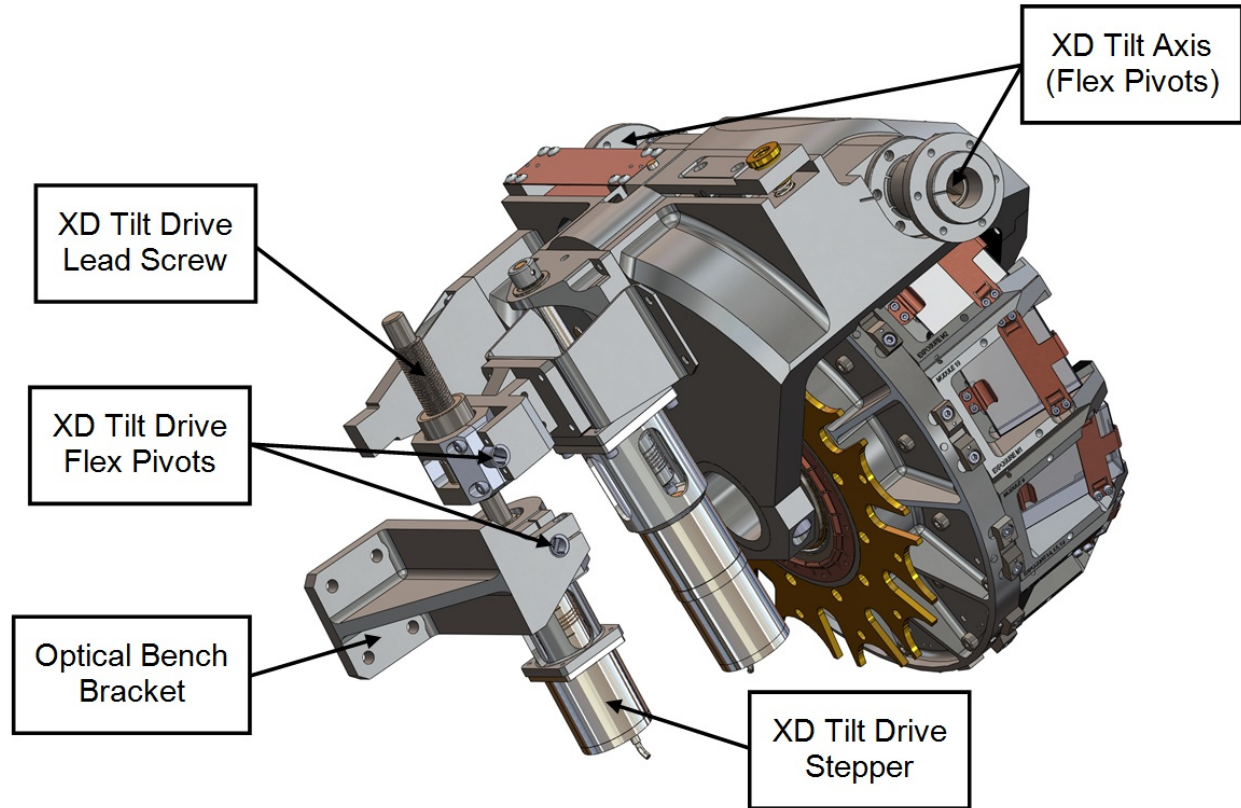


Figure #26: XDM Tilt Mechanism

### 6.2.2 Tilt Drive:

The cross disperser tilt drive consists of a lead screw with an ACME thread that engages with an anti-backlash split nut to provide continuous adjustment over the angular range of travel. A Phytron stepper motor rated for a cryogenic, high vacuum environment is used to drive the lead screw. Hard stops will be implemented to limit that angular travel of the XD tilt axis in both directions.

(Note: An ACME thread profile is preferable over a square thread profile because it allows the split nut to clamp over the threads to remove backlash and it is preferable over an ANSI screw thread because the shallow thread angle causes less frictional force for power transmission.)



### 6.2.3 Tilt Angle Control:

#### 6.2.3.1 Choice of a type of sensor:

(Note: for the complete analysis, see Technical Note.)

#### Hall Effect Sensor (F.W. Bell FH-301-040):

Pros	Cons
<ul style="list-style-type: none"> <li>- Price</li> <li>- Already implemented in SpeX</li> <li>- Passive Sensing. Can be used simultaneously with Detector Readout.</li> </ul>	<ul style="list-style-type: none"> <li>- Unknown Accuracy</li> <li>⇒ Too much effort needed to quantify at the level of accuracy required.</li> <li>- Range is limited. "Physical range reduction trick" (*) isn't applicable.</li> <li>- No package or mount included.</li> <li>- Potential irregular magnetization</li> </ul>



#### Eddy Current Sensor (Kaman DIT-5200L / 20N):

Pros	Cons
<ul style="list-style-type: none"> <li>- Known accuracy.</li> <li>- Comes as a set: Sensors + Electronics.</li> <li>- Extremely Linear.</li> <li>- Range can be tuned using a "Physical range reduction trick". (*)</li> <li>- Easier to implement</li> </ul>	<ul style="list-style-type: none"> <li>- Price.</li> <li>- Needs Coax cables.</li> <li>- Active sensor: can perturb detector readout.</li> <li>- Needs 10/15 minutes to warm up and give reliable data after turning it on =&gt; RF switch needed.</li> </ul>

(\*) The "Physical Range Reduction Trick" Can only be used with an active sensor and a passive target (aluminum). See (6.2.2.2).

Considering ease of implementation, cost, risks and performances, the choice of going with the Kaman is largely preferred.

Ease of implementation because the "physical range reduction trick" can be used (See 6.2.2.2) but also because the sensor package is threaded for easy mounting. (Unlike the Hall-effect sensor that needs to be epoxied).

As for the other criteria, it is important to note that no data is available in regards to the Hall-effect sensor accuracy. Since the accuracy needed for the Cross-Disperser mechanism is much higher than the focus stage in SpeX, the stage mechanism cannot be used as a benchmark. In order to make sure that the Hall effect sensor's performance is sufficient, it would then be necessary to "verify in the lab". However, due to the very high accuracy, it would be very costly to implement such a test setup. Since the accuracy data is available for the Kaman sensor and exceeds the requirements with a comfortable safety factor, it is clear that the difference of retail cost of the sensor is no longer an argument.

### 6.2.3.2 Physical Range Reduction

Thanks to the fact that Eddy Current sensors don't need to use magnetic targets but only conductive ones, basically only the minimum distance between the sensor and the target is being sensed. In the case of a Hall-effect sensor, what is sensed is the magnetic field of the target. And since the magnetic field isn't homogeneous, it is necessary for the center of the target to be aligned with the center of the sensor. Because of that fact, it would be pretty much impossible to implement the system as described in the Figure below with a Hall Effect sensor.

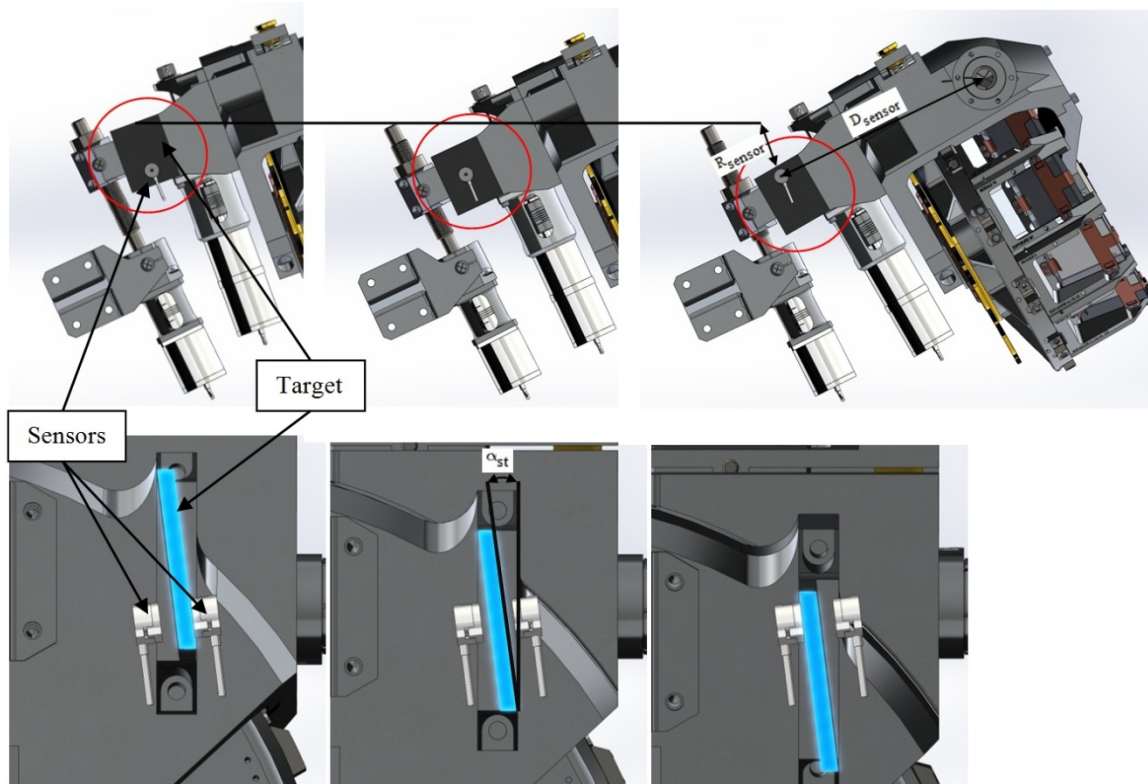


Figure #27: “Physical Range Reduction” in the Cross-Disperser Mechanism

## 7 Discrete Linear Position Mechanisms

### 7.1 The Dekker Concept:

#### 7.1.1 Mask Dimensions

Based on the requirements of 4 Slit Lengths described in (5.2.1.1), see below (figure #XXXX) the slit openings on the Dekker mask and their dimensions:

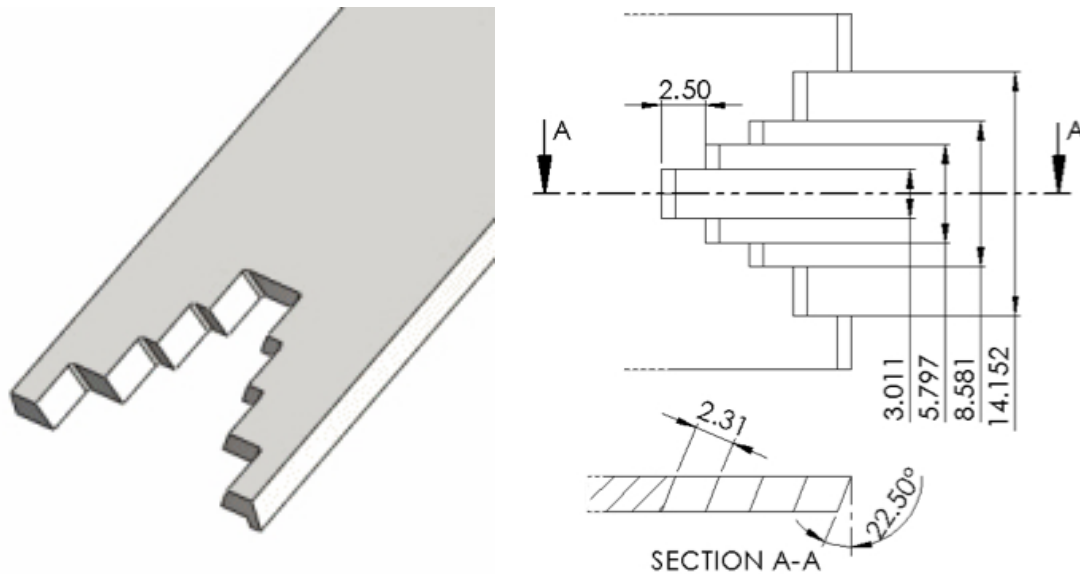


Figure #28: Dekker Mask Dimensions

Note that the openings are tilted 22.5 degrees in order to be parallel to the light beam. Each of the slit length openings is 2.5mm wide on the mask front face, which correspond to a 2.31mm opening for the beam. Considering the widest slit on the Slit Mirror, the maximum width of the beam will be 1.658mm. The main advantage of having an opening of about .65mm wider than the beam is to reduce substantially the precision needed on the translation axis of the mask. The mask however, will need to be positioned very precisely on the axis perpendicular to the translation axis of the mask.

#### 7.1.2 Original Concept: Miniature X-stage

##### 7.1.2.1 Stage Description

In order to precisely translate the Dekker mask into its 4 discrete positions, and to allow the Dekker mechanism to fit between the Slit wheel and the Order Sorting wheel, the choice has been oriented toward the use of a low profile piezo-stage. It is important to note that the choice

of a piezo-stage versus a traditional translation stage (with a stepper motor) wasn't driven by the precision requirement but by the necessity to keep the stage as small as possible. After an extensive research, it appeared that the only supplier able to deliver an off-the-shelf low profile piezo-stage that is qualified for cryogenic temperatures (~77K) was MICOS GmbH. Among their selection of products, the best candidate is the PPS-20. See figure #XXX below:

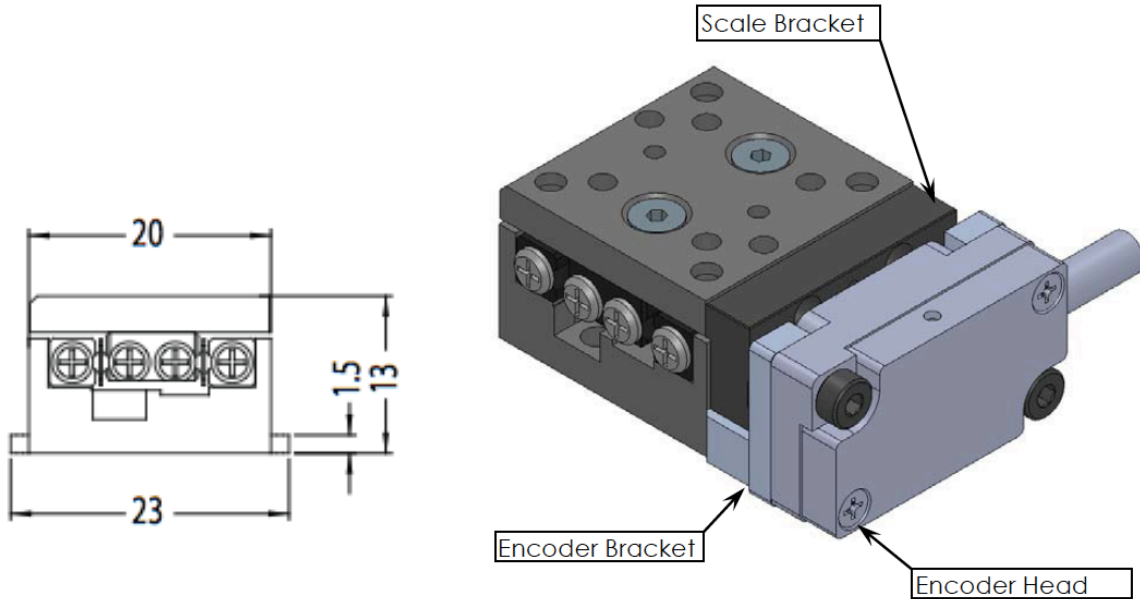
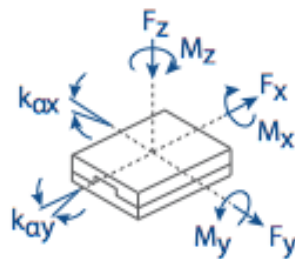


Figure #29: MICOS PPS-20 cryogenic piezo X-stage

The MICOS PPS-20 has a 12mm travel range. It is utilizing a dual piezo motor for increased precision and the stage is guided in translation with two precision ball slides with a 1µm preload. At ambient temperature (25C) the stage is rated for a maximum speed of 2mm/sec and a 1nm precision in open loop. Under these conditions, it is rated for the following loads:

Load, max	$F_x$ [N]	$F_y$ [N]	$F_z$ [N]	$M_x$ [N·m]	$M_y$ [N·m]	$M_z$ [N·m]	$k_{ax}$ [µrad/N·m]	$k_{ay}$ [µrad/N·m]
PM-002	2	20	20	0.7	0.7	0.7	-	-



Under cryogenic temperature, the piezo material is generally “less efficient”, so it is a good assumption to de-rate by 50% the data above (load, speed, and precision). At this point, we are waiting to get more precise info from the manufacturer, based on their test data. In addition, the stage is rated for an expected life between 2500m and 5000m of translation. Again, this is to be confirmed with the manufacturer at this point.

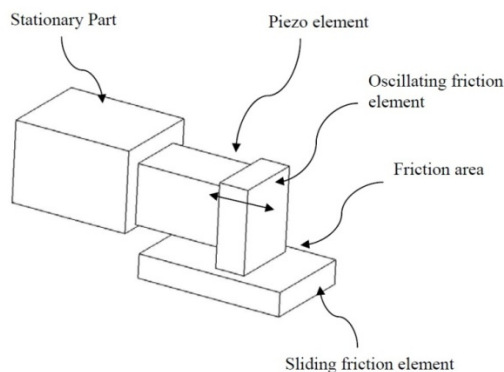
Another important point to consider is the necessity to have a stage that doesn’t generate any heat when stopped in position and that will stay in position in case of power outage. Since a piezo is basically a capacitor with a minor resisting loss, it doesn’t create any actual power, unless there is a varying voltage going through it. At standstill, there is no variation of voltage and therefore no heat dissipation. And actually in case of a power outage, the stage will freeze in position and have its regular load capacity.

For the position feedback, the manufacture provides an encoder that can operate at cryogenic temperature.

#### Stick Slip Principle:

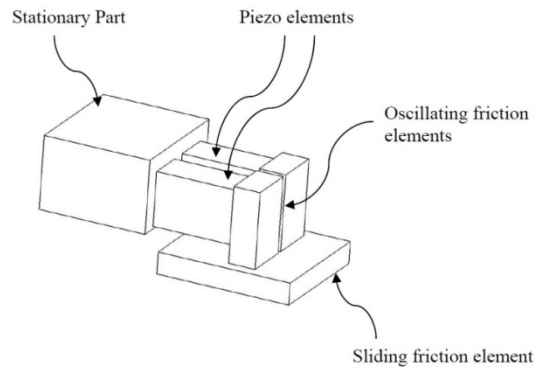
The piezo motor of the PPS-20 stage is using the Stick-Slip (Inertial) principle.

The basic principle of the stick-slip inertial motion is the controlled use of the moving part’s inertia and friction. As shown in the drawing below, a piezo element is connected to an oscillating friction element, which moves the sliding friction element forward when the piezo extends due to an applied voltage. When the piezo is fully extended, which is usually bellow 1um, a fast voltage transition is applied that quickly contracts the piezo resulting in a fast backwards motion of the oscillating friction element. This processed is repeated until the sliding friction element, which is usually attached to the moving part of the positioner, reaches its desired position.



The main problem with the conventional stick-slip piezo motors described above is that the sliding friction element follows the backwards movement to some degree during the slip phase, which results in poor velocity regulation, induced vibration into the system, and lost motion (slower velocity and lower efficiency).

In order to significantly these undesired “side-effects”, MICOS is using a so-called Multi-phase Stick-Slip piezo motor, which lessens or completely eliminates the backward motion during the slip phase. This MICOS piezo-motor utilizes 2 piezos and friction elements that move in unison, but slip at different times. Using that method, at least one element reduces or eliminates the retract motion. See figure #?? Below:



### 7.1.2.2 Piezo-Stage Testing:

In order to increase the level of confidence that we could rely on this new technology, we decided that it would be highly preferable to test the piezo-stage. The test planned was including cryogenic and vacuum test, position hold test, re-initialization test, hard-stop test and lifecycles. Unfortunately, so far we were not able to operate the stage at 77K. We might be able to solve the issues if we invest more time in the troubleshooting, however due the critical path schedule we decided that it was necessary to design a “fall back” concept. (See 7.1.3)

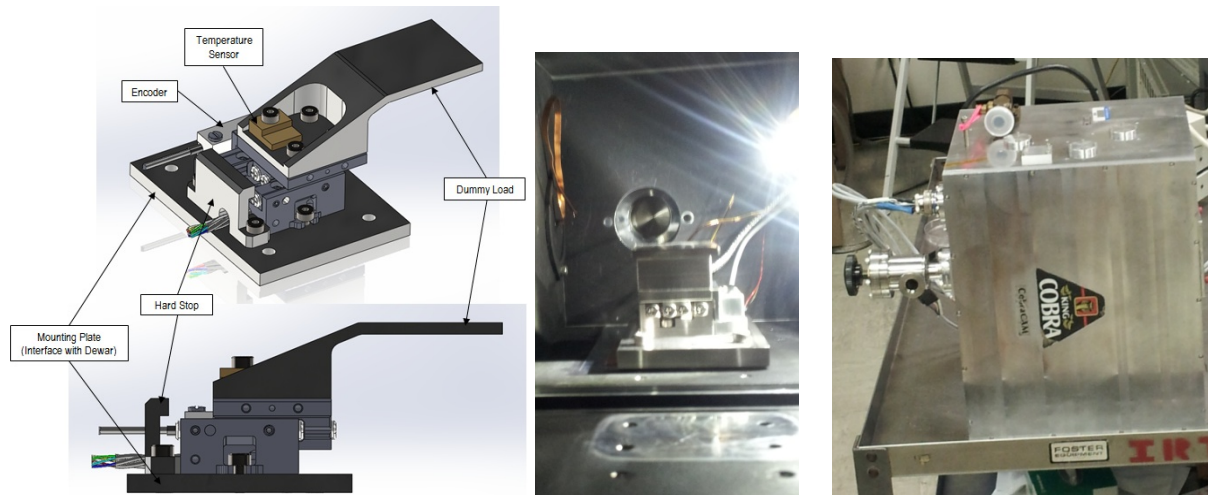


Figure #30: Piezo X-stage test setup

### 7.1.3 Alternative Concept:

#### 7.1.3.1 Description:

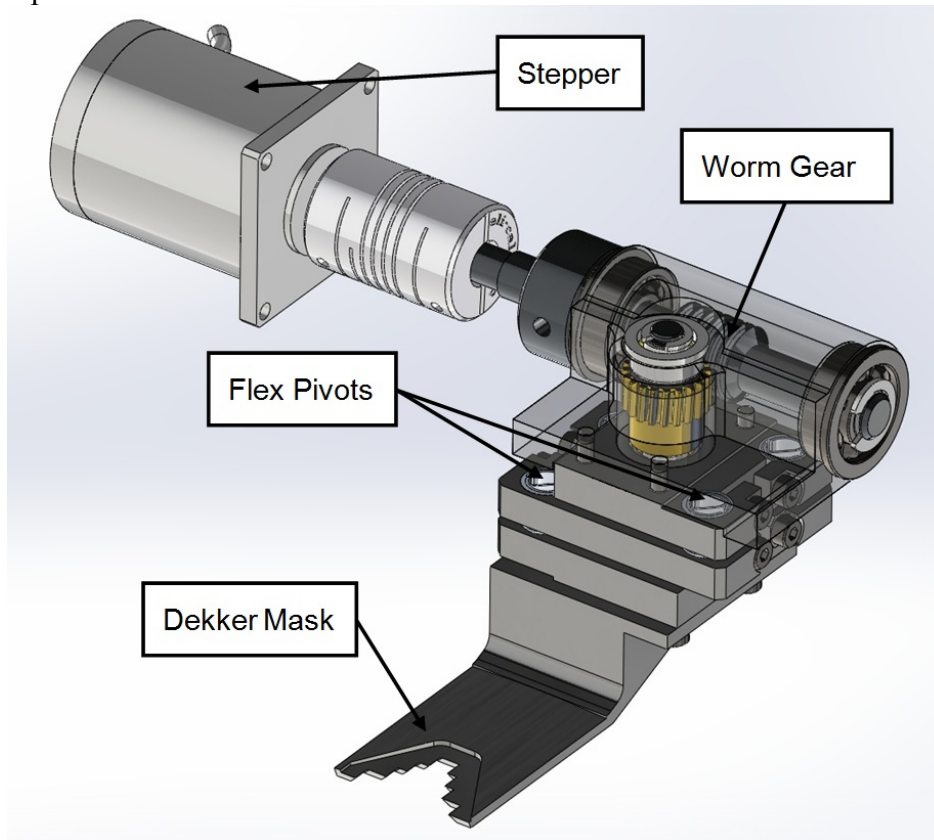


Figure #31: Dekker Flexure Mechanism

As an alternative concept to the Piezo-Stage, a Flexure Stage actuated with an eccentric and driven by a Worm Gear / Stepper was developed. The Flexure Stage is designed using 2 parallel arms attached with flex-pivots, on one side to the mask carriage and on the other to the fixed base. The eccentric is pushing the mask carriage in translation.

In reality, due to the non-symmetric configuration of the Flexure, the carriage will not only translate on X but also slightly on Y. However, for this particular functionality, it is not a problem because the mask can be cut in a way that will compensate for the Y-translation.

This alternative concept the advantage to be inherently more reliable but also it will be easier to isolate the Stepper from the light path. With the Piezo-Stage it is trickier because the radiating element (the Piezo Motor) is within the stage.

### 7.1.3.2 Cinematic

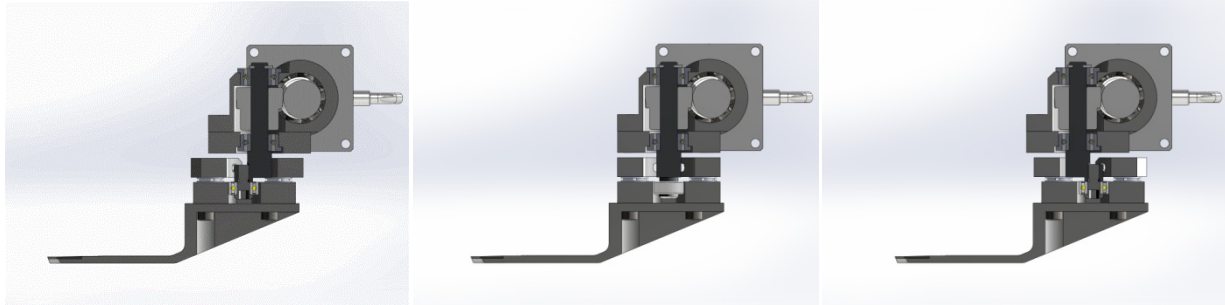


Figure #32: Dekker Flexure Mechanism – Eccentric Cinematic

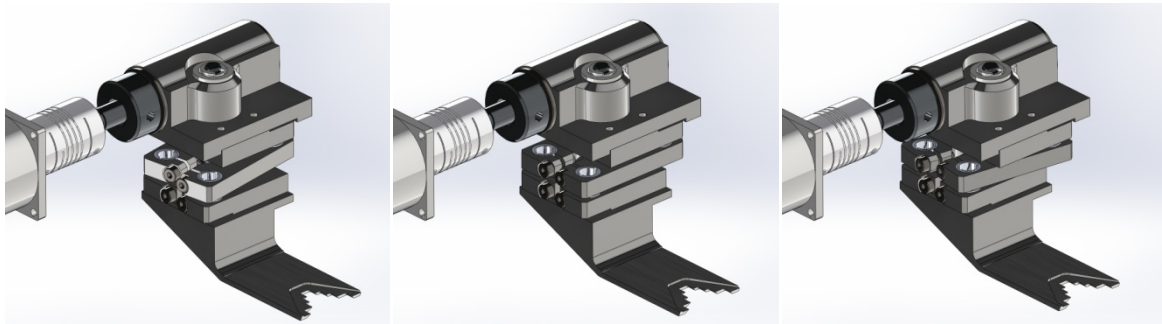


Figure #33: Dekker Flexure Mechanism – Flexure Cinematic

## 7.2 The Immersion Grating (IG) Mechanism

The optical design calls for an Immersion Grating element after the first off-axis parabola (OAP1).

The light beam entering the spectrometer is first filtered through the Order Sorting filter, then folded on the sixth fold mirror (FM6) and collimated at OAP1. In fact, the optical design requires having the choice of two different R3 silicon immersion gratings (IG1 and IG2) located at the pupil following OAP1. In order to select either of the 2 IGs, the two IGs will be mounted at 90deg from each other and an in/out mirror mechanism located close to the pupil will redirect the beam toward the desired IG.

### 7.2.1 Immersion Gratings Mounts Concept

Each of the Immersion Grating elements shall be held in a statically determined manner using 3 points of contact and maintained in position using springs.

Temperature Control: (See Thermal Requirements Document:.....)

*“Precision temperature control of the two immersion gratings requires that the two gratings be sufficiently thermally isolated from the cold structure to allow temperature control without the need for large heat inputs. Since the cool down time gets longer with increased thermal isolation the required thermal impedance is a trade off between heat input and cooling rate.”*

At the light of the thermal calculations, it appears that the best option to control the IG’s temperature is to isolate them from the Bench using G-10 legs and then, to thermally connect them back to the bench using copper straps. Then, depending on the temperature sensor reading, heater resistors will be used in order to increase the temperature in case it had dropped under a certain temperature threshold. This method will allow to closed-loop control the temperature setpoint. See Figure below that illustrates the different components of the IG mounts.

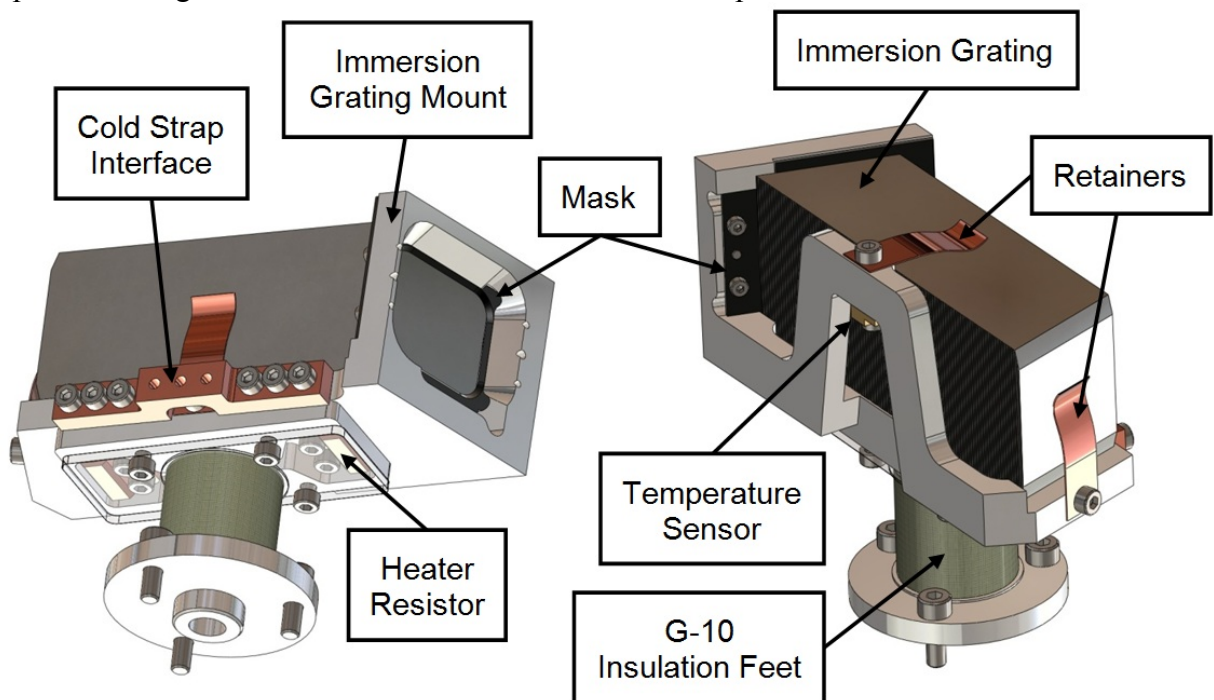


Figure #34: Immersion Grating Mount Description

Remark: the IG requiring the most precise positioning should be located at the “out position” of the folding mirror.

---

## 7.2.2 In/Out Fold Mirror Concept

### 7.2.2.1 Optical Elements

The only optical element in the In/Out fold mirror mechanism is the fold mirror itself. The size of the mirror is determined by the size of the beam being reflected on it. But since the beam is “getting smaller” as it approaches the pupil, the further away the fold mirror will be located from the pupil, the bigger the fold mirror will have to be.

Also, the mirror will only be used to fold the beam 90deg toward IG2, so the mirror will be oriented 45deg from the centerline of the beam coming from OAP1. The 45deg tilt implies that the mirror width will have to be larger than the beam at the fold point multiplied by a factor  $\cos(45\text{deg})$ .

### 7.2.2.2 Choice of a type of mechanism:

There are basically two main types of mechanisms that can be used for an In/Out mirror mechanism. Either a flip system with the mirror mount rotating on an axis, or a translation system.

The choice of the type of mechanism here is mostly driven by the space available and with a goal to optimize the volume of the mechanism. Also, the face of the mirror needs to be located very precisely, so the use of a stop parallel to the mirror is highly desirable.

For the concept, the first approach was to use an off-the-shelf cryogenic translating stage that would come in and out of the beam perpendicularly to the mirror. See figure #2.

The advantage of translating perpendicularly to the mirror is the possibility to push the mirror on its stop perpendicularly. However, since the mirror is angled 45deg to the beam, the travel of the beam is increased by a factor of  $\sqrt{2}$  in comparison to coming perpendicularly to the beam. The increase of travel also requires a longer and wider stage. Not only this is against the goal of optimizing the volume of the mechanism but also the fact that the stage is wider obliges to locate the mirror further away from the pupil in order to clear the IG with the stage. Then, since the beam size increases as it is further from the pupil, a wider mirror would be necessary, which again increases the travel needed. Finally, with the mirror being further away from the pupil, IG2 can no longer be on the slit viewer side of the beam because of the Order Sorting wheel, so it would have to be located on the spectrometer side of the beam.

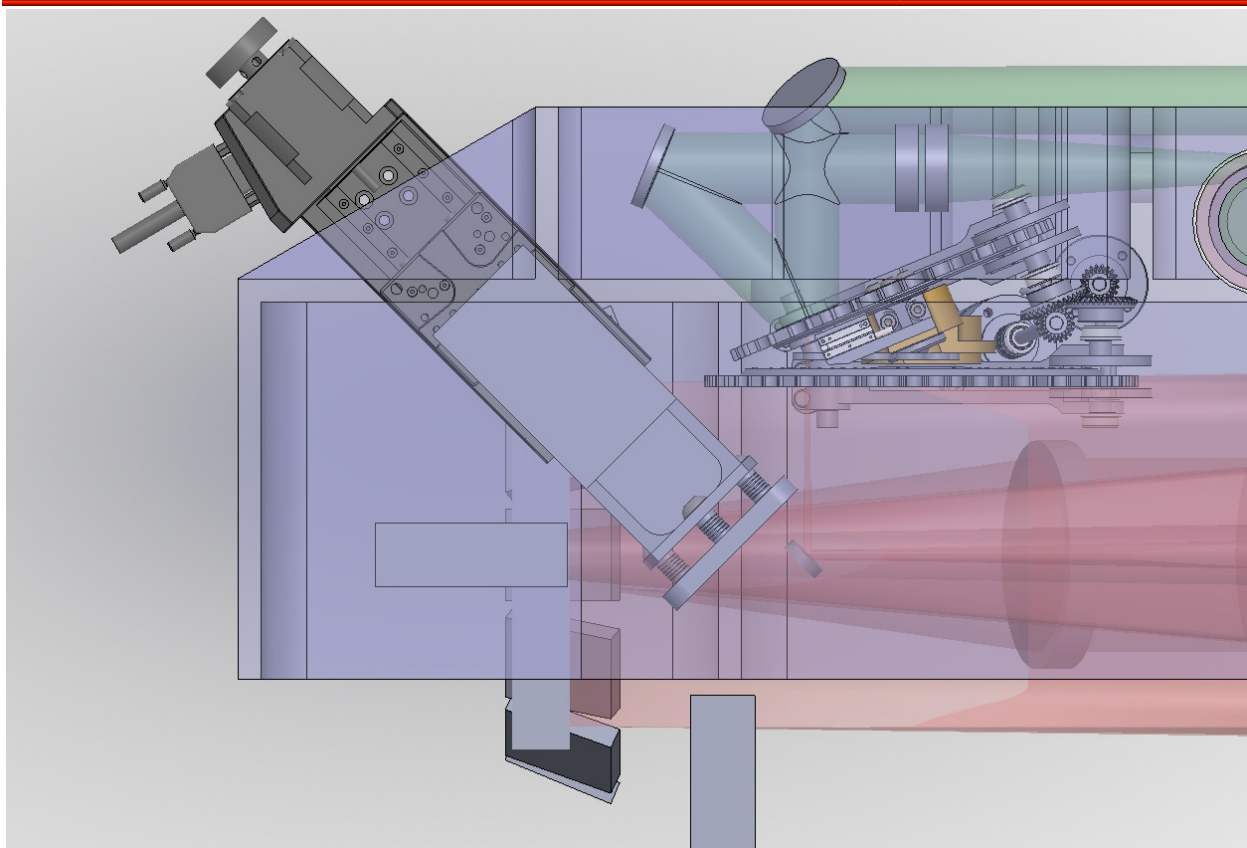


Figure #35: translating stage perpendicular to the mirror (Earlier Concept)

So, although a translating stage seems ideal to position the mirror against its stop, it turned out to be highly space consuming.

Another investigated alternative was to use a flip mirror. But for similar reasons, like clearing the IGs, it turned out to be also problematic.

The best alternative chosen for the second concept was then to use a translating stage coming perpendicularly to the beam. See 7.2.2.3 for more details.

### 7.2.2.3 Description of the In/Out Mechanism

The pictures below (Figure #3 and #4) illustrate the 2 positions of the In/Out mechanism that was chosen:

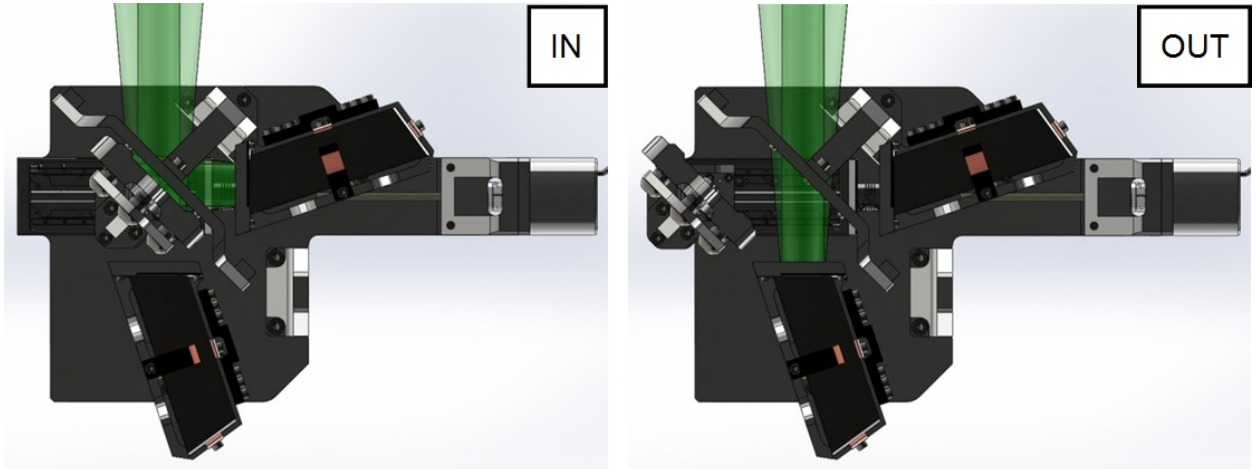


Figure #36: In/Out Fold Mirror

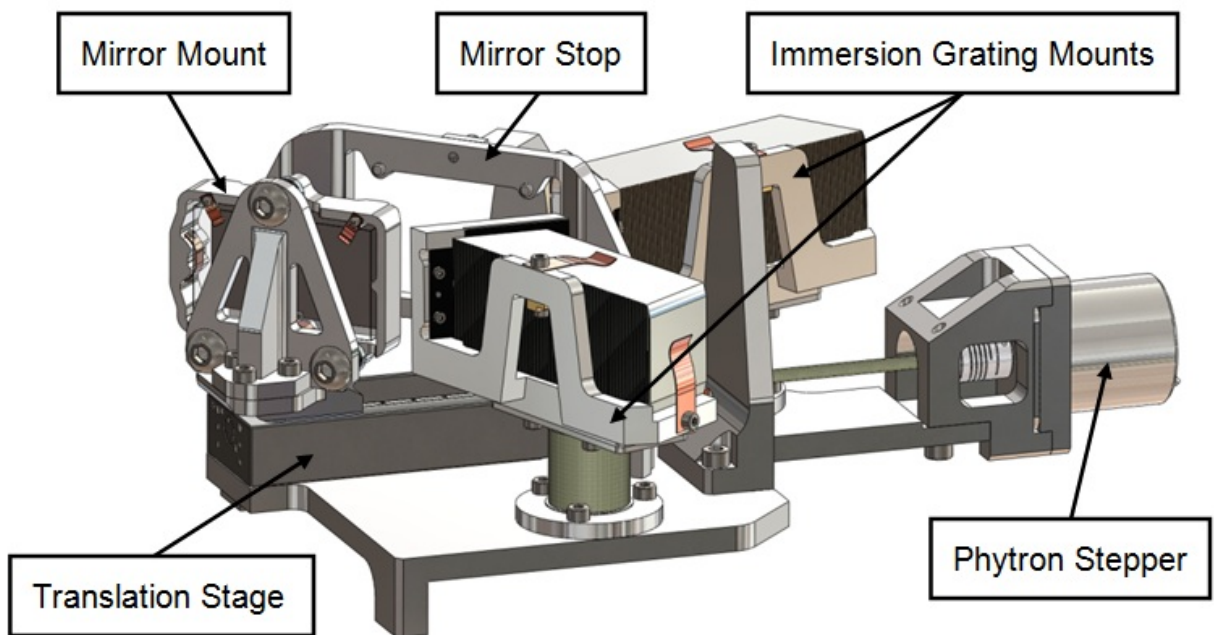


Figure #37: In/Out Fold Mirror - Description

With the stage perpendicular to the beam, the mirror cell comes in contact at 45deg to the mirror stop.

The challenge resides in being able to properly statically determinate the mirror on the stop. A good way to achieve it is to spring load the mirror against the stop. The 3 machined springs in the model are utilized to spring load the mirror cell against the stop but also to give it 6 degrees of freedom so that only the stop determinates the position, not the translation stage. This way, the position of the face of the mirror is guaranteed to be precise on its normal axis, the Z-axis, but also in rotation around the X-axis and the Y-axis. Finally, it is optically less important for the mirror to be precisely located on its 3 others degrees of freedom, so that setup is sufficient.

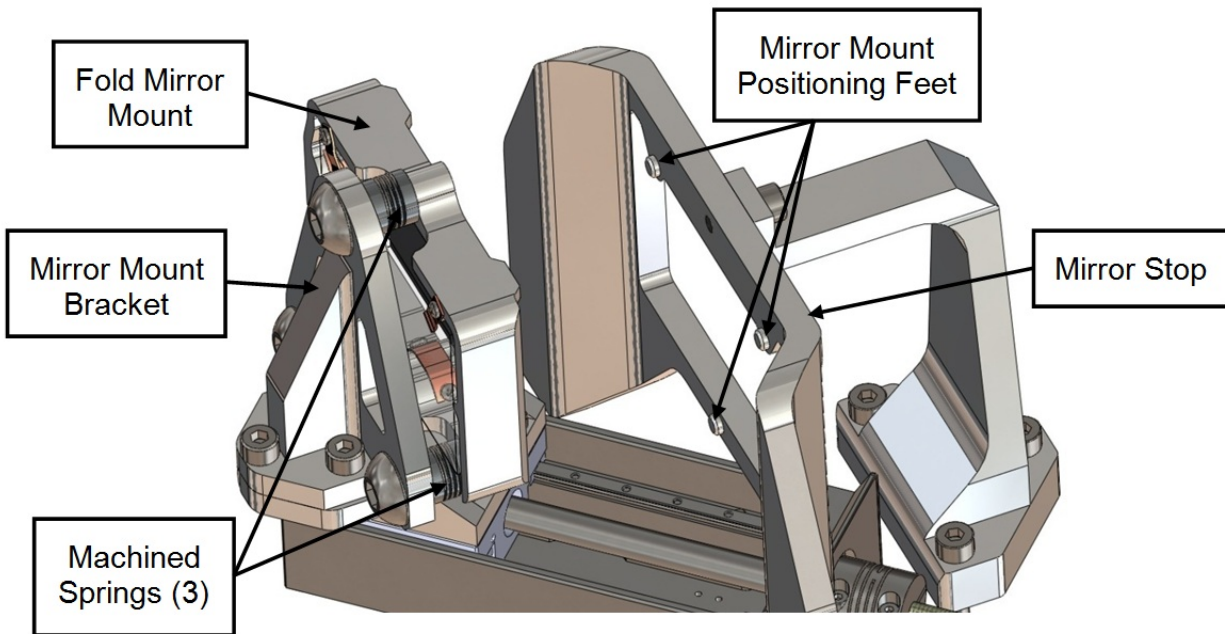


Figure #38: Preloaded Mirror and Mirror Stop

Remark: ideally, the mirror would be in contact with the 3 feet of the stop. However it is to be avoided because the feet would very likely damage the mirror. So instead, the mirror is first held in position in the cell (See 3.3.5) and then the cell is positioned against the stop. (The cell has 3 “ears” for the contact with the mirror stop.)

#### The Translation Stage:

For the In/Out mechanism concept, we were able to find an off-the-shelf translating stage that is rated for cryogenic temperatures. The stage that was chosen is a MICOS LS-40. For the cryogenic version, MICOS is using an off-the-shelf cryogenic stepper from Phytron, the VSS-32.

Using an off-the-shelf stage has an obvious cost advantage, but also, the fact that a Phytron stepper drives this particular stage is an important plus. Indeed, we decided to standardize on using Phytron steppers from the VSS series for all of the other mechanisms from iSHELL where steppers are required. Among others, one significant advantage of standardizing our steppers is the minimization of control strategies and software development. So choosing a stage driven by a Phytron stepper is coherent with our strategy.

Also, we have confirmed that the holding force of the stage with power turned off will be sufficient to retain the mirror mount spring loaded against the stop. The use of a power-off brake shouldn't be necessary.

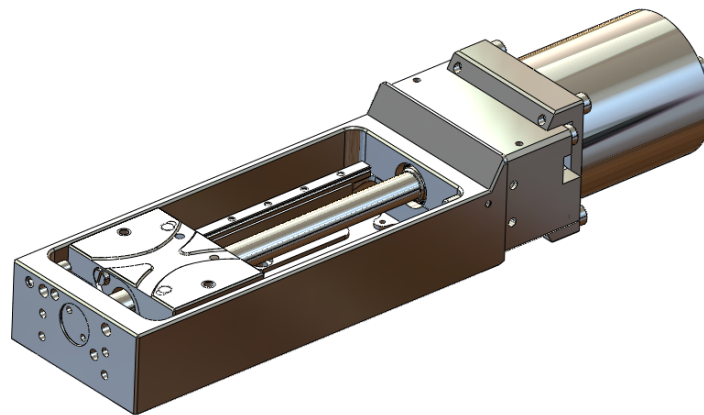


Figure #39: MICOS LS-40 translation stage

#### 7.2.2.4 Discrete Position Feedback

A Hall Effect Sensor will be utilized in order to verify the position of the stage in each of its 2 discrete positions. For more details refer to .....

7.2.2.5 Fold Mirror mount:

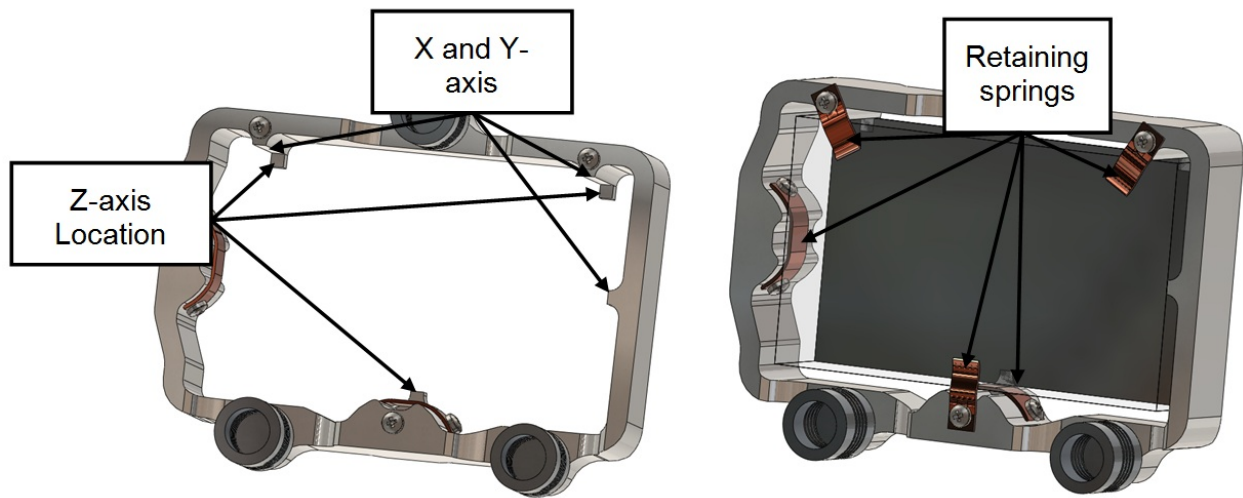
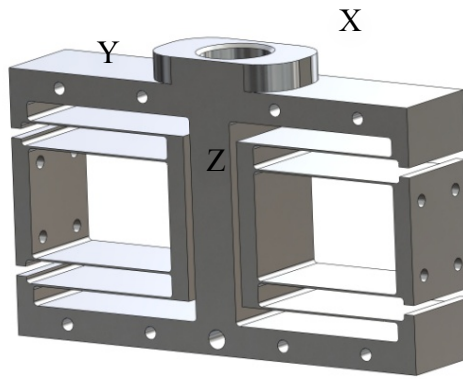


Figure #40: Fold Mirror Cell

The fold mirror is located in translation on the Z-axis and in rotation around X and Y thanks to the 3 Z-axis location feet of the cell. The 3 points will statically determinate the mirror. In the same way, the 3 X and Y-axis location feet will statically determinate the mirror, locating it in translation on the X and Y-axis and in rotation around the Z-axis. The mirror will be held in position using 5 springs as represented on the figure above.

## 8 Continuous Linear Position Mechan

### 8.1 The Spectrograph Detector Focus S



The optical design calls for a 2048x2048 H2RG array at the end of the spectrograph. The array requires to be mounted on a precise focus stage.

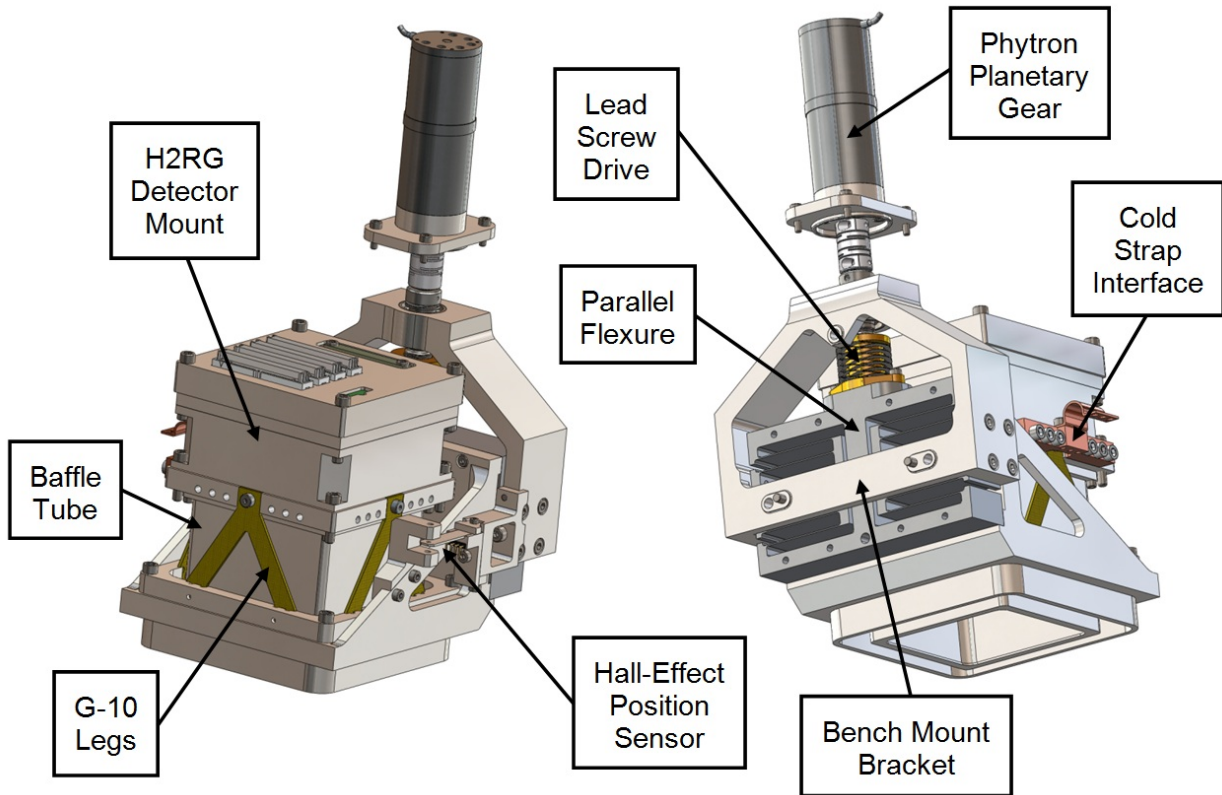
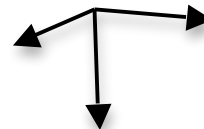
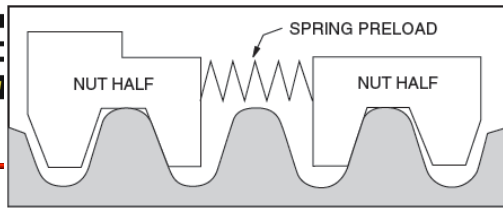


Figure #41: Spectrograph Detector Focus Stage Description

Just like for SpeX's focus stage, it appears evident that the use of a Parallel Flexure is a proven solution that should also be used for iSHELL. The flexure has the advantage to be highly rigid on TX, TY, RX, RY and RZ while allowing a very precise positioning along TZ. The flexure is driven using a lead screw.





In order to precisely position the spectrograph detector along the Z-axis, the driving lead screw needs to have as little backlash as possible.

The standard method for taking up backlash is to bias two nut halves axially using some type of compliant spring.

The unit is very stiff in the direction in which the nut half is loaded against the flank of the screw thread. However, in the direction away from the screw thread, the nut is only as axially stiff as the amount of preload that the spring exerts.

For example, if the maximum axial load to which the system is subjected is 50 lbs., the amount of spring preload must be equal to, or greater than, 50 lbs. in order to maintain intimate screw/nut contact. Therefore, in iSHELL's design, the preload provided by wave-spring must be greater than the axial load of the flexure and the detector mount. (See Calculation Document.....)

Note: the problems arising from preloading in this manner are increased drag torque and nut wear.

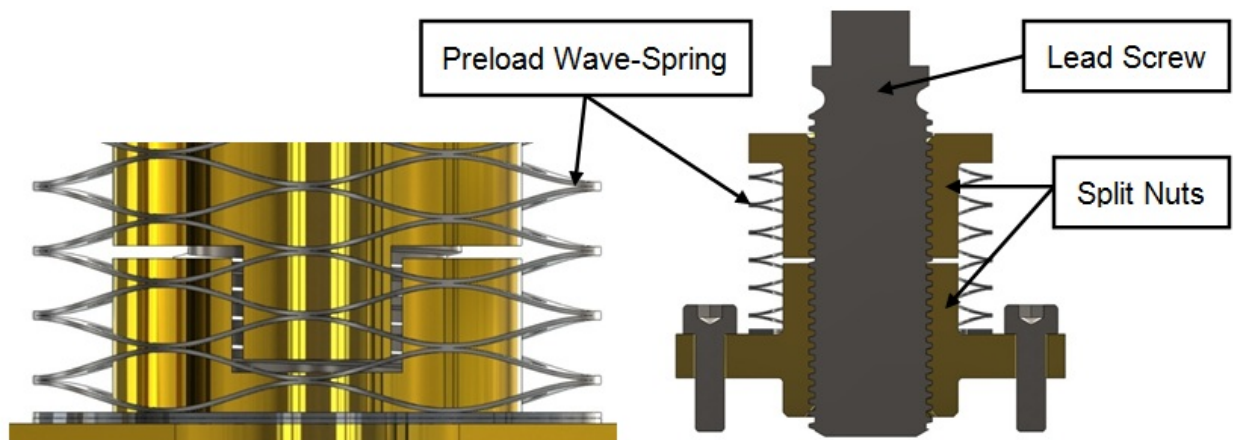


Figure #42: Focus Stage Anti-Backlash System